



Submitted to: Physics Letters B



CERN-PH-EP-2015-143
28th June 2015

Measurement of the production of neighbouring jets in lead-lead collisions at $\sqrt{s_{\text{NN}}} = 2.76$ TeV with the ATLAS detector

The ATLAS Collaboration

Abstract

This Letter presents measurements of correlated production of nearby jets in Pb+Pb collisions at $\sqrt{s_{\text{NN}}} = 2.76$ TeV using the ATLAS detector at the Large Hadron Collider. The measurement was performed using 0.14 nb^{-1} of data recorded in 2011. The production of correlated jet pairs was quantified using the rate, $R_{\Delta R}$, of “neighbouring” jets that accompany “test” jets within a given range of angular distance, ΔR , in the pseudorapidity–azimuthal angle plane. The jets were measured in the ATLAS calorimeter and were reconstructed using the anti- k_t algorithm with radius parameters $d = 0.2, 0.3,$ and 0.4 . $R_{\Delta R}$ was measured in different Pb+Pb collision centrality bins, characterized by the total transverse energy measured in the forward calorimeters. A centrality dependence of $R_{\Delta R}$ is observed for all three jet radii with $R_{\Delta R}$ found to be lower in central collisions than in peripheral collisions. The ratios formed by the $R_{\Delta R}$ values in different centrality bins and the values in the 40–80% centrality bin are presented.

Measurement of the production of neighbouring jets in lead–lead collisions at $\sqrt{s_{\text{NN}}} = 2.76$ TeV with the ATLAS detector

Abstract

This Letter presents measurements of correlated production of nearby jets in Pb+Pb collisions at $\sqrt{s_{\text{NN}}} = 2.76$ TeV using the ATLAS detector at the Large Hadron Collider. The measurement was performed using 0.14 nb^{-1} of data recorded in 2011. The production of correlated jet pairs was quantified using the rate, $R_{\Delta R}$, of “neighbouring” jets that accompany “test” jets within a given range of angular distance, ΔR , in the pseudorapidity–azimuthal angle plane. The jets were measured in the ATLAS calorimeter and were reconstructed using the anti- k_t algorithm with radius parameters $d = 0.2, 0.3$, and 0.4 . $R_{\Delta R}$ was measured in different Pb+Pb collision centrality bins, characterized by the total transverse energy measured in the forward calorimeters. A centrality dependence of $R_{\Delta R}$ is observed for all three jet radii with $R_{\Delta R}$ found to be lower in central collisions than in peripheral collisions. The ratios formed by the $R_{\Delta R}$ values in different centrality bins and the values in the 40–80% centrality bin are presented.

1. Introduction

Experimental studies of jet production in Pb+Pb collisions at the LHC can directly reveal the properties of the quark–gluon plasma created in the collisions. One predicted consequence of quark–gluon plasma formation is “jet quenching” that refers to the modification of parton showers initiated by hard-scattering processes which take place in the quark–gluon plasma [1]. Measurements of jet pairs at the LHC provided the first direct evidence of jet quenching [2, 3]. In those measurements, the enhancement of transverse momentum imbalance of dijets in central Pb+Pb collisions was observed. Measurements at the LHC of inclusive jet suppression [4, 5] and the variation of the suppression with jet azimuthal angle with respect to the elliptic flow plane [6] have shown that the transverse energy of jets is significantly degraded and that the energy loss depends on the path length of the parton shower in the plasma. These dijet and single-jet measurements provide complementary information about the jet quenching process. The single jet measurements are sensitive to the average partonic energy-loss while the dijet measurements probe differences in the quenching between the two parton showers traversing the medium. Those differences can arise from the unequal path lengths of the showers in the medium or from fluctuations in

the energy loss process itself.

To help disentangle the contributions of these factors to the observed dijet asymmetries, the measurement of the correlations between jets that are at small relative angles was performed. Neighbouring jet pairs include jets originating from the same hard interaction, but also jets from different hard interactions. The latter are not of interest in this analysis, and are subtracted statistically. The remaining neighbouring jet pairs result primarily from hard radiation by the parton that occurs early in the process of the shower formation. Generally, two neighbouring jets originating from the same hard scattering should have more similar path lengths in the medium compared to the two jets in the previous dijet measurement. Therefore measuring neighbouring jets could probe differences in their quenching that do not result primarily from difference in path length. More generally, measurements of the correlated production of jets in the same parton shower may provide more detailed insight into the modification of the parton shower in the quark–gluon plasma beyond the subsequent quenching of the resulting jets.

This Letter presents measurements of the production rate of neighbouring jets in Pb+Pb collisions at $\sqrt{s_{\text{NN}}} = 2.76$ TeV characterized by the quantity $R_{\Delta R}$ introduced in Ref. [7]. The $R_{\Delta R}$ vari-

able quantifies the rate of neighbouring jets that accompany “test” jets within a given range of angular distance, ΔR , in the pseudorapidity–azimuthal angle (η – ϕ) plane¹, where $\Delta R = \sqrt{(\Delta\eta)^2 + (\Delta\phi)^2}$. Jets were reconstructed with the anti- k_t [8] algorithm using radius parameter values $d = 0.2, 0.3$, and 0.4 . In events with test jets with transverse energy $E_T > 70$ GeV, further jets are searched for within a certain angular distance from the test jet.

The rate of the neighbouring jets that accompany a test jet, $R_{\Delta R}$, is defined as

$$R_{\Delta R}(E_T^{\text{test}}, E_T^{\text{nbr}}) = \frac{\sum_{i=1}^{N_{\text{jet}}^{\text{test}}} N_{\text{jet},i}^{\text{nbr}}(E_T^{\text{test}}, E_T^{\text{nbr}}, \Delta R)}{N_{\text{jet}}^{\text{test}}(E_T^{\text{test}})}, \quad (1)$$

where E_T^{test} and E_T^{nbr} are the transverse energies of the test and neighbouring jet, respectively; $N_{\text{jet}}^{\text{test}}$ is the number of test jets in a given E_T^{test} bin and $N_{\text{jet}}^{\text{nbr}}$ is the number of neighbouring jets. Further, the $R_{\Delta R}$ quantity was used to define per-test-jet normalized spectra of neighbouring jets as

$$\frac{dR_{\Delta R}}{dE_T^{\text{nbr}}} = \frac{1}{N_{\text{jet}}^{\text{test}}} \sum_{i=1}^{N_{\text{jet}}^{\text{test}}} \frac{dN_{\text{jet},i}^{\text{nbr}}}{dE_T^{\text{nbr}}}(E_T^{\text{test}}, E_T^{\text{nbr}}, \Delta R). \quad (2)$$

Previous measurements of the correlated production of neighbouring jets were performed by the D0 experiment in $p\bar{p}$ collisions at the Tevatron [7]. The measurements by D0 were intended to measure the strong coupling constant, α_s , and to test its running over a large range of momentum transfers. The measurements presented in this Letter use similar techniques and follow notations introduced in that measurement.

2. Experimental setup

The measurements presented in this Letter were performed using the ATLAS inner detector, calorimeter, trigger and data acquisition systems [9]. The inner detector [10] measures charged

particles within the interval $|\eta| < 2.5$. The inner detector is composed of silicon pixel detectors in the innermost layers, followed by silicon microstrip detectors and a straw-tube tracker, all immersed in a 2 T axial magnetic field provided by a solenoid. The calorimeter system consists of a high-granularity liquid argon (LAr) electromagnetic (EM) calorimeter covering $|\eta| < 3.2$, a steel/scintillator sampling hadronic calorimeter covering $|\eta| < 1.7$, a LAr hadronic calorimeter covering $1.5 < |\eta| < 3.2$. The hadronic calorimeter has three sampling layers longitudinal in shower depth and has a $\Delta\eta \times \Delta\phi$ granularity of 0.1×0.1 for $|\eta| < 2.5$ and 0.2×0.2 for $2.5 < |\eta| < 4.9$.² The EM calorimeters are segmented into three shower-depth compartments with an additional pre-sampler layer. The forward regions are instrumented with copper/LAr and tungsten/LAr forward calorimeters (FCal) covering $3.2 < |\eta| < 4.9$, optimised for electromagnetic and hadronic energy measurements, respectively. Two minimum-bias trigger scintillators (MBTS) counters are located on each side at 3.56 m along the beamline from the centre of the ATLAS detector. The MBTS detect charged particles in the range $2.1 < |\eta| < 3.9$. Each MBTS counter is divided into 16 sections, each of which provides measurements of both the pulse heights and arrival times of energy deposits. The zero-degree calorimeters (ZDCs) are located symmetrically at $z = \pm 140$ m and cover $|\eta| > 8.3$. In Pb+Pb collisions the ZDCs measure primarily “spectator” neutrons, which originate from one of the incident nuclei and do not interact hadronically with nucleons of the other nucleus.

Minimum-bias Pb+Pb collisions were required either to have the transverse energy in the whole calorimeter exceeding 50 GeV at the Level-1 trigger or to have a track reconstructed in the inner detector in coincidence with ZDC signals on both sides.

Events with high- p_T jets were selected using a combination of a minimum-bias Level-1 trigger and High Level Trigger (HLT) jet triggers. The Level-1 minimum-bias trigger required a total transverse energy measured in the calorimeter to be larger than 10 GeV. The HLT jet trigger used the offline Pb+Pb jet reconstruction described in Section 4, except for the application of the final hadronic energy scale correction. The HLT jet trigger selected

¹ ATLAS uses a right-handed coordinate system with its origin at the nominal interaction point (IP) in the centre of the detector and the z -axis along the beam pipe. The x -axis points from the IP to the centre of the LHC ring, and the y axis points upward. Cylindrical coordinates (r, ϕ) are used in the transverse plane, ϕ being the azimuthal angle around the beam pipe. The pseudorapidity is defined in terms of the polar angle θ as $\eta = -\ln \tan(\theta/2)$.

²An exception is the third sampling layer that has a segmentation of 0.2×0.1 up to $|\eta| = 1.4$.

events containing a $d = 0.2$ jet with $E_T > 20$ GeV.

3. Event selection and data sets

This analysis used data from Pb+Pb collisions at a nucleon–nucleon centre-of-mass energy of $\sqrt{s_{\text{NN}}} = 2.76$ TeV recorded by ATLAS in 2011. It utilizes data samples corresponding to a total integrated luminosity of 0.14 nb^{-1} . The minimum-bias sample was recorded with different prescales depending on the instantaneous luminosity in the LHC fill. The prescale indicates which fraction of events that passed the trigger selection were selected for recording by the DAQ. The minimum-bias trigger recorded an effective luminosity of $7 \mu\text{b}^{-1}$. Events selected by the minimum-bias trigger and the jet triggers were required to have a reconstructed primary vertex with at least three associated tracks each with $p_T > 500$ MeV and a difference between time of pulses from the two sides of the MBTS detector of less than 7 ns. A total of 51 (14.2) million minimum-bias triggered (jet-triggered) events passed the applied event selections and were used in the analysis.

In heavy ion collisions, “centrality” reflects the overlap volume of the two colliding nuclei, controlled by the impact parameter of the collisions. The centrality of Pb+Pb collisions was characterized by ΣE_T^{FCal} , the total transverse energy measured in the FCal [11]. The centrality intervals were defined according to successive percentiles of the ΣE_T^{FCal} distribution ordered from the most central (highest ΣE_T^{FCal}) to the most peripheral collisions. Production of neighbouring jets was measured in four centrality bins: 0–10%, 10–20%, 20–40%, and 40–80%, with the 40–80% bin serving as the reference. The percentiles were defined after correcting the ΣE_T^{FCal} distribution for a 2% minimum-bias trigger inefficiency that affects the most peripheral events, which are not included in this analysis.

The performance of the ATLAS detector and offline analysis in measuring jets in the environment of Pb+Pb collisions was evaluated using a large sample of Monte Carlo (MC) events obtained by overlaying simulated PYTHIA [12] hard-scattering events onto randomly selected minimum-bias Pb+Pb events, recorded by ATLAS during the same data-taking period as the data used in this analysis. PYTHIA version 6.423 with the AUET2B tune [13] was used. Three million PYTHIA events were produced for each of five intervals of the transverse momentum of outgoing partons in the

$2 \rightarrow 2$ hard-scattering process, with boundaries 17, 35, 70, 140, 280, and 560 GeV. The detector response to the PYTHIA events was simulated using GEANT4 [14, 15], and the simulated hits were combined with the data from the minimum-bias Pb+Pb events before performing the reconstruction.

4. Jet reconstruction and neighbouring jet selection

Jets were reconstructed within the pseudorapidity interval $|\eta| < 2.8$. The jet reconstruction techniques described in Ref. [4] were used, and are briefly summarized here. The anti- k_t algorithm was first run in four-vector recombination mode, on $\Delta\eta \times \Delta\phi = 0.1 \times 0.1$ logical towers. The energies in the towers were obtained by summing energies of calorimeter cells, calibrated at a scale set for electron showers, within the tower boundaries. Then, an iterative procedure was used to estimate a calorimeter layer- and η -dependent underlying event (UE) energy density, while excluding actual jets from that estimate. The UE energy was subtracted from each calorimeter cell within the towers included in the reconstructed jet. The subtraction accounted for a $\cos 2\phi$ modulation in the UE energy density due to collective flow [11] of the medium using a measurement of the amplitude and phase of that modulation in the calorimeter. The jet energies and momenta were calculated via a sum of all cells contained within the jets, treating each cell as a massless four-vector, using E_T values after the UE subtraction. A correction was applied to the reconstructed jet transverse energies to account for jets not excluded or only partially excluded from the UE estimate. The magnitude of the correction was typically a few percent but can be as large as 10% for jets whose energies are fully included in the UE estimate. Then, a final η - and jet E_T -dependent hadronic energy scale calibration factor was applied [4].

Separate from the calorimeter jets, “track jets” were reconstructed by applying the anti- k_t algorithm with $d = 0.4$ to charged particles having $p_T > 4$ GeV. The track jets were used in conjunction with electromagnetic clusters to remove the contribution of “UE jets” generated by fluctuations in the underlying event. The technique is described in detail in Ref. [4].

In the MC simulation, the kinematics of the reference PYTHIA generator-level jets (hereafter called “truth jets”) were reconstructed from PYTHIA

final-state particles with the anti- k_t algorithm with radius $d = 0.2, 0.3$, and 0.4 using the same techniques as applied in pp analyses [16]. PYTHIA truth jets were matched to the closest reconstructed jet of the same d value within $\Delta R = 0.2$. The resulting matched jets were used to evaluate the jet energy resolution (JER), the jet energy scale (JES), the jet angular resolution, and the jet reconstruction efficiency.

The $R_{\Delta R}$ measurement was performed with the sample triggered by the jet triggers. The measurement was done differentially in transverse energy of the test and neighbouring jets, and in collision centrality. Five E_T^{test} intervals 70–80, 80–90, 90–110, 110–140, 140–300 GeV and four E_T^{nbr} intervals, 30–45, 45–60, 60–80, 80–130 GeV were used. Furthermore configurations where all the E_T bins of the test jets or of the neighbouring jets have the same upper bound of 300 GeV were also used in this analysis. The number of bins and their boundaries were chosen to minimize the impact of the limited number of events in the data while preserving the ability to infer the trends in the measured distributions. For each jet radius, neighbouring jets are considered if they lie within a specific annulus in ΔR around the test jet: $0.5 < \Delta R < 1.6$, $0.6 < \Delta R < 1.6$, and $0.8 < \Delta R < 1.6$ for $d = 0.2$, $d = 0.3$, and $d = 0.4$ jets, respectively. The inner edge of each annulus was chosen to avoid possible overlap of test and neighbouring jets, and the outer edge value ($\lesssim \pi/2$) rejects neighbouring jets in the hemisphere opposite to the test jet and maximizes the number of events. Choosing a maximum ΔR of 1.6 restricts the pseudorapidity range of test jets to $|\eta| < 1.2$, yielding approximately 87×10^3 $d = 0.4$ test jets with $p_T > 80$ GeV analysed in 0–10% central events and 37×10^3 test jets in 40–80% peripheral events.

To quantify the centrality dependence of the neighbouring jet yields, the ratio $\rho_{R_{\Delta R}} \equiv R_{\Delta R}|_{\text{cent}}/R_{\Delta R}|_{40-80}$ is calculated as the ratio of $R_{\Delta R}$ measured in each centrality bin to $R_{\Delta R}$ measured in the reference (40–80%) bin.

5. Corrections to neighbouring jet rates

The raw rates of neighbouring jets include a contribution from neighbouring jets that originate from different hard partonic interactions in the same Pb+Pb collision. This combinatorial background is present both in the MC simulation and in the data and must be subtracted. It is largest in the low E_T^{nbr}

bins and it increases with increasing centrality of the collision, since the probability for the presence of two independent hard scatterings in one Pb+Pb collision is expected to increase with the number of binary collisions. The combinatorial background is estimated using the differential yield of inclusive jets ($d^3 N_{\text{jet}}/d\eta d\phi dE_T$) evaluated in minimum-bias Pb+Pb events. To each event considered a weight is assigned such that the event sample obtained from the minimum-bias trigger has the same centrality distribution as the sample collected by the jet trigger. This estimated background needs to be corrected for a geometrical bias present in the case where the combinatorial jet overlaps with a real neighbouring jet or when two combinatorial jets overlap. These biases were removed by applying a multiplicative correction factor to background distributions prior to the subtraction. This multiplicative factor was derived from the reconstruction efficiency of two neighbouring jets evaluated as a function of their angular separation in the annulus. In that evaluation, one jet was required to originate from PYTHIA’s hard scattering and the other jet was required to originate from the minimum-bias data in the overlay. The impact of this correction on the final subtracted distribution is smaller than 0.5%.

The combinatoric jet kinematics may also be affected by the presence of a test jet. To control this influence, a study comparing the combinatoric jets from the overlay MC events with the same jets in the original minimum-bias data was performed. This study resulted in an additional correction, independent of centrality and jet E_T , that decreases the combinatorial background by 1.5%. The $\pm 1.2\%$ uncertainty on the correction originates from the limited number of events and was included in the systematic uncertainties.

In order to account for the effect of the azimuthal dependence of jet yields [6], the combinatorial background was reweighted to take into account the measured azimuthal distributions of test jets as well as combinatorial jets. The change of the raw subtracted distribution in central collisions and low E_T^{nbr} bins after the reweighting is at the level of 1% and decreases with increasing centrality of the collision and E_T^{nbr} .

The background is subtracted from raw $R_{\Delta R}$ distributions both in the data and in the MC simulation, allowing an evaluation of the effectiveness of the subtraction using the MC simulation. The signal-to-background ratio strongly depends on the

centrality of the collision and E_T^{nbr} . In 0–10% central collisions, the signal-to-background ratio can be as low as 0.15 for the most extreme case of $30 < E_T^{\text{nbr}} < 45$ GeV, and increases to approximately 0.8 for $60 < E_T^{\text{nbr}} < 80$ GeV.

The raw subtracted $R_{\Delta R}$ distributions are affected by the jet energy resolution. The combination of the jet energy resolution and the steeply falling E_T spectrum produces a net migration of jets from lower E_T to higher E_T values such that a jet reconstructed with a given E_T^{rec} corresponds, on average, to a lower truth jet E_T , $\langle E_T^{\text{truth}} \rangle$. The relationship between $\langle E_T^{\text{truth}} \rangle$ and E_T^{rec} was evaluated in simulated events for the different centrality bins and three jet radii used in the analysis. The extracted relationships were used to correct for the average shift in the test jet energy. No correction due to the jet reconstruction efficiency for the test jets is needed, since the analysis operates in the transverse energy region where the jet reconstruction is fully efficient. No correction due to jet trigger efficiency is needed either since the plateau of the jet trigger efficiency is reached for all test jets, except for $d = 0.4$ jets with $E_T^{\text{test}} < 90$ GeV in the 0–10% and 10–20% centrality bins. In the region $70 < E_T < 90$ GeV, the jet trigger efficiency is above 85%. A systematic uncertainty is applied to describe the effect of the lower jet reconstruction efficiency.

The impact of the jet energy resolution, reconstruction efficiency, and angular resolution on neighbouring jet yields is corrected for by applying bin-by-bin unfolding to the raw subtracted $R_{\Delta R}$ distributions. For each measured $R_{\Delta R}$ distribution, two corresponding MC distributions are evaluated, one using truth jets and the other using jets after the detector simulation. The ratio of these two MC distributions provides a correction factor which is then applied to the data.

The bin-by-bin correction factors are derived from the MC simulation where the reconstructed jets were matched to the truth jets. To account for the impact of the jet angular resolution, the truth jet is required to lie within a given annulus while the reconstructed jet is allowed to fall outside of the annulus.

Examples of jet reconstruction efficiencies for neighbouring jets and the bin-by-bin correction factors are shown in Fig. 1 for different centrality selections and for two choices of jet radii: $d = 0.4$ and $d = 0.2$. Generally, the jet energy resolution in central (0–10%) collisions for $d = 0.4$ jets has compa-

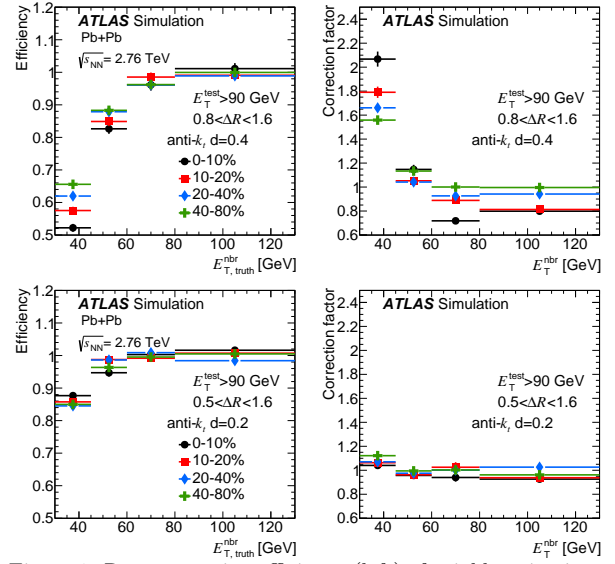


Figure 1: Reconstruction efficiency (left) of neighbouring jets as a function of the transverse energy of the neighbouring jet at Monte Carlo generator level $E_{T,\text{truth}}^{\text{nbr}}$ and bin-by-bin correction factors for the distributions of the neighbouring jet rate $R_{\Delta R}$ (right) as a function of the reconstructed transverse energy of the neighbouring jet E_T^{nbr} . Plots for two different jet radii, $d = 0.4$ (upper plots) and $d = 0.2$ (lower plots) are shown and the transverse energy of the test jet E_T^{test} is required to exceed 90 GeV. The four different centrality bins are denoted by different markers in each plot. The vertical error bars represent statistical uncertainties.

rable contributions from UE fluctuations and the “intrinsic” resolution of the calorimetric jet measurement. The fluctuations in the UE are approximately two times smaller for $d = 0.2$ jets than they are for $d = 0.4$ jets. Thus, the distributions measured using $d = 0.2$ jets are far less sensitive to the effects of the jet energy resolution, and consequently the resulting bin-by-bin correction factors for those distributions exhibit only a modest centrality dependence. The difference in the jet reconstruction efficiency between the two choices of jet radii is also significant – the efficiency for $d = 0.2$ jets plateaus around 30 GeV, where it is still rising rapidly for $d = 0.4$ jets.

The jet angular resolution is determined in MC simulation as the standard deviation of the difference in angles between truth and reconstructed jets. In both η and ϕ it reaches 0.008 in 0–10% collisions and 0.005 in the 40–80% centrality bin for $d = 0.4$ jets with $E_T = 30$ GeV. The angular resolution improves with increasing jet E_T and reaches 0.004 (resolution in η) and 0.002 (resolution in ϕ) at $E_T = 200$ GeV, independently of centrality.

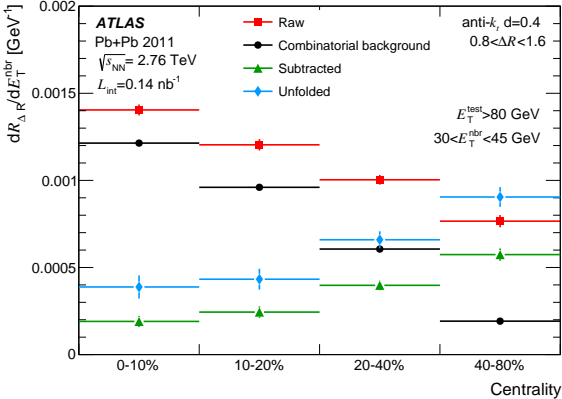


Figure 2: Summary of how the corrections impact the $dR_{\Delta R}/dE_T^{nbr}$ distribution measured in the data in different centrality bins. The $dR_{\Delta R}/dE_T^{nbr}$ is shown for $d = 0.4$ jets for $E_T^{test} > 80$ GeV and in the interval $30 < E_T^{nbr} < 45$ GeV. Squares show the raw $dR_{\Delta R}/dE_T^{nbr}$ prior to the UE subtraction, circles show the combinatorial background, triangles show the subtracted $dR_{\Delta R}/dE_T^{nbr}$ prior to unfolding by applying the bin-by-bin correction factors, and diamonds show the unfolded $dR_{\Delta R}/dE_T^{nbr}$. Vertical error bars on the combinatorial background, raw, and subtracted distributions represent statistical uncertainties. Vertical error bars on the unfolded distribution represent the combined statistical uncertainty from the unfolding and from subtracted distributions.

The impact of these corrections on $R_{\Delta R}$ distributions measured in the data in different centrality bins is shown in Fig. 2. The figure shows the raw $R_{\Delta R}$ distribution, and the combinatorial background, subtracted, and final unfolded $R_{\Delta R}$ distributions for $d = 0.4$ jets with $E_T^{test} > 80$ GeV and in the lowest E_T^{nbr} interval, $30 < E_T^{nbr} < 45$ GeV. The raw $R_{\Delta R}$ distribution increases from peripheral to central collisions. The increase of the combinatorial background is steeper than the increase of the raw distribution. Therefore, a decrease of subtracted $R_{\Delta R}$ with increasing collision centrality is observed. The shape of the $R_{\Delta R}$ distribution remains unchanged when the bin-by-bin correction is applied.

6. Systematic uncertainties

Systematic uncertainties in the measurement of $R_{\Delta R}$ distributions and their ratios, $\rho_{R_{\Delta R}}$, arise from the uncertainty on the jet energy scale, jet energy resolution, angular resolution, bin-by-bin unfolding, centrality, combinatorial background and jet trigger efficiency. The impact of uncertainties on the jet energy scale, jet energy resolution and jet

angular resolution was assessed by constructing new bin-by-bin correction factors with a systematically varied relationship between the reconstructed and truth jet kinematics. The resulting uncertainties on $R_{\Delta R}$ and $\rho_{R_{\Delta R}}$ were evaluated from their changed values obtained with modified jet energy scale, jet energy resolution and jet angular resolution dependencies.

The systematic uncertainty due to the jet energy scale is composed of two parts: an absolute, centrality-independent component, and a centrality-dependent component. The uncertainty on $R_{\Delta R}$ from the jet energy scale uncertainty is evaluated by shifting all reconstructed jet transverse energies by ± 1 standard deviation of the jet energy scale uncertainty. The absolute component is determined from the *in situ* studies of the calorimeter response; systematic variations of the jet response in the MC simulation [16]; and from studies of the relative energy scale difference between the jet reconstruction procedure in heavy-ion collisions, and the procedure used for inclusive jet measurements in 2.76 TeV and 7 TeV pp collisions [17]. The magnitude of the uncertainty on the $R_{\Delta R}$ from the absolute jet energy scale uncertainty varies from 2% to 15% as a function of E_T and radius of the jet. The centrality-dependent component of jet energy scale uncertainty [5] was estimated using the PYQUEN MC generator [18] to provide a sample of jets with modified fragmentation functions consistent with measurements in quenched jets performed by ATLAS [19] and CMS [20].

The centrality-dependent jet energy scale uncertainty reaches 1% for 0–10% central collisions and less than 0.25% for 40–80% peripheral collisions. The uncertainty on $R_{\Delta R}$ originating from the centrality-dependent component of the jet energy scale uncertainty increases from less than 1% in peripheral collisions to 3% in central collisions.

The effect of the jet energy resolution uncertainty was evaluated by applying modified bin-by-bin correction factors where the reconstructed jet E_T was smeared. The uncertainty on the jet energy resolution is dominated by the uncertainty in the detector response. Thus, the procedure used for jet measurements in the 7 TeV pp collisions [16] is used. The smearing factor is evaluated using an *in situ* technique involving studies of dijet energy balance. The systematic uncertainty on $R_{\Delta R}$ due to the jet energy resolution varies from 1% to 4% depending on the jet E_T . The centrality-independent jet energy

scale uncertainty and the uncertainty from jet energy resolution tend to cancel in the $\rho_{R_{\Delta R}}$ ratios since both the numerator and denominator in the ratios are affected to a similar degree by the variations accounting for the uncertainties.

The systematic uncertainty on combinatorial contributions originates from the previously noted uncertainty on the correction factor taking into account the difference between jets in minimum-bias events and combinatorial jets in the overlay. The resulting uncertainty reaches $\sim 8\%$ in 0–10% central collisions at low E_T^{nbr} and rapidly decreases with decreasing centrality or increasing E_T^{nbr} .

The systematic uncertainty associated with the bin-by-bin unfolding is connected with possible differences in the spectral shape between the data and the MC simulation. To achieve better correspondence with the data, the simulated jet spectrum was reweighted to match the spectral shape in the data before deriving the bin-by-bin correction factors as described above. Conservatively, the entire change in $R_{\Delta R}$ and $\rho_{R_{\Delta R}}$ induced by the use of reweighted bin-by-bin correction factors is taken as a systematic uncertainty. Typically, this results in 1–2% uncertainty on $R_{\Delta R}$. A maximum uncertainty of 5% is reached in 0–10% central collisions for $R_{\Delta R}$ evaluated for neighbouring jets with $E_T^{\text{nbr}} > 30$ GeV.

The uncertainty on the centrality estimation originates from the uncertainty on the estimated inefficiency of the minimum-bias trigger. The analysis was repeated with modified centrality bins assuming 100% minimum-bias trigger efficiency. The resulting uncertainty is typically smaller than 5% with a mild E_T dependence and a negligible centrality dependence.

The uncertainty associated with the jet angular resolution is estimated using modified bin-by-bin correction factors where the reconstructed jet η and ϕ is smeared to reflect a up to $\sim 15\%$ centrality and E_T dependent uncertainty on the angular resolution. The uncertainty on the jet angular resolution was estimated by comparing the angular distance between track jets and the closest calorimetric jet in the data and in the MC simulation. The magnitude of uncertainty on $R_{\Delta R}$ from the jet angular resolution is smaller than 2%.

The systematic uncertainty on the jet trigger efficiency covers a possible bias caused by selecting test jets in the region where the jet trigger is not fully efficient. This is the case for the $d = 0.4$ jets with $E_T^{\text{test}} < 90$ GeV reconstructed in the 0–10% and 10–20% centrality bins. For that E_T region, the

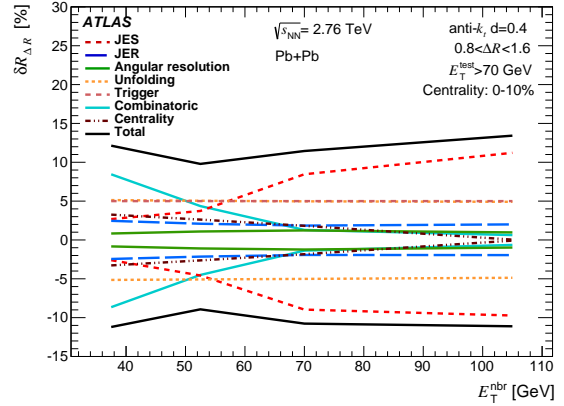


Figure 3: Summary of the relative systematic uncertainties, in %, on the $R_{\Delta R}$ distributions ($\delta R_{\Delta R}$). The systematic uncertainties due to the jet energy scale (JES), the jet energy resolution (JER), the jet angular resolution, unfolding, jet trigger efficiency, combinatorial contributions and centrality are shown for $d = 0.4$ jets with $E_T^{\text{test}} > 70$ GeV in 0–10% central collisions.

systematic uncertainty was determined as the difference between the trigger efficiencies for inclusive jets and jets that were required to have a neighbouring jet. This trigger efficiency difference is less than 5% and is independent of the E_T^{nbr} .

To avoid statistical fluctuations in the values of systematic uncertainties, the weak E_T^{nbr} dependence of the uncertainties is smoothed by a second-order polynomial. Systematic uncertainties on $R_{\Delta R}$ for $d = 0.4$ jets are summarized in Table 1 for the 0–10% and 40–80% centrality bins. The table shows the maximum values of uncertainties for $R_{\Delta R}$ and for $\rho_{R_{\Delta R}}$. The total systematic uncertainties for jets with the other two jet radii are smaller than those shown in the table. For the 0–10% centrality bin these systematic uncertainties are also plotted in Fig. 3 as a function of E_T^{nbr} .

7. Results

The $R_{\Delta R}$ measurement is performed differentially in collision centrality, transverse energy of the test jet, E_T^{test} , and transverse energy of the neighbouring jet, E_T^{nbr} , as described Sec. 4. The measured distributions are divided into four centrality bins, 0–10%, 10–20%, 20–40%, and 40–80%. Fig. 4 shows the fully corrected $R_{\Delta R}$ distributions for $d = 0.4$ and $d = 0.2$ jets evaluated as a function of E_T^{test} . The distributions are shown for four centrality bins and three different lower bounds on the

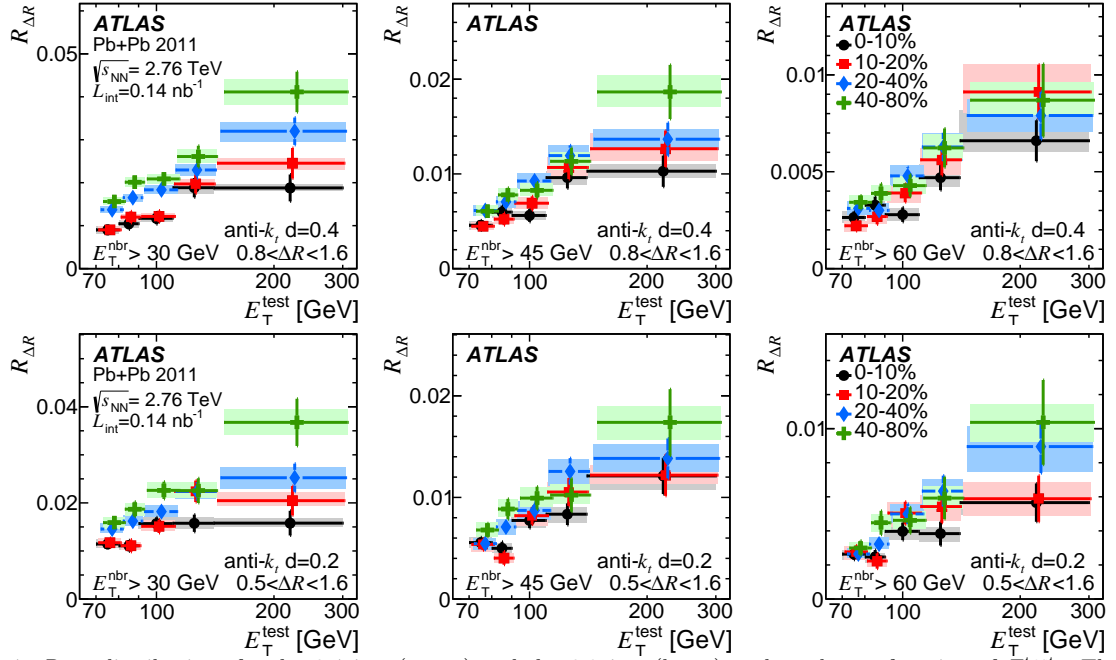


Figure 4: $R_{\Delta R}$ distributions for $d = 0.4$ jets (upper) and $d = 0.2$ jets (lower) evaluated as a function of E_T^{test} . The three different columns show $R_{\Delta R}$ distributions evaluated for three different lower bounds on the neighbouring-jet transverse energy, $E_T^{nbr} > 30, 45$, and 60 GeV. The four different centrality bins are denoted by different markers in each plot. The shaded bands indicate systematic uncertainties, vertical error bars represent statistical uncertainties. The data points and horizontal uncertainties for the $10\text{--}20\%$, $20\text{--}40\%$, and $40\text{--}80\%$ centrality bins are shifted along the horizontal axis with respect to the $0\text{--}10\%$ centrality bin for clarity.

	$\delta R_{\Delta R}$		$\delta \rho_{R_{\Delta R}}$
	0–10%	40–80%	0–10%
JES	15%	11%	7 %
JER	4%	2%	2%
Angular resolution	2%	0.5%	2%
Unfolding	5%	2%	5%
Centrality	6%	6%	6%
Combinatoric	8%	<0.5%	8%
Trigger	5%	—	5%

Table 1: Maximum systematic uncertainties on $R_{\Delta R}$ ($\delta R_{\Delta R}$) and on the ratio of $R_{\Delta R}$ in central collisions and in peripheral (40–80%) collisions $\rho_{R_{\Delta R}}$ ($\delta \rho_{R_{\Delta R}}$) for $d = 0.4$ jets in the 0–10% and 40–80% centrality bins. The systematic uncertainty on the trigger is applicable only for $E_T^{test} < 90$ GeV.

neighbouring-jet transverse energy, $E_T^{nbr} > 30, 45$, and 60 GeV. The shaded error bands on the plots indicate the systematic uncertainties discussed in Section 6. The $R_{\Delta R}$ distribution exhibits an increase with increasing E_T^{test} . Sizeable differences between the four different centrality bins are observed for all three jet radii. The yield of neigh-

	0–10%
$d = 0.4$	$2.73 \pm 0.23(stat.) \pm 0.12(syst.)$
$d = 0.3$	$2.83 \pm 0.16(stat.) \pm 0.14(syst.)$
$d = 0.2$	$2.81 \pm 0.15(stat.) \pm 0.15(syst.)$
	10–20%
$d = 0.4$	$2.85 \pm 0.17(stat.) \pm 0.13(syst.)$
$d = 0.3$	$2.51 \pm 0.15(stat.) \pm 0.11(syst.)$
$d = 0.2$	$2.56 \pm 0.16(stat.) \pm 0.12(syst.)$
	20–40%
$d = 0.4$	$2.90 \pm 0.12(stat.) \pm 0.10(syst.)$
$d = 0.3$	$2.91 \pm 0.11(stat.) \pm 0.09(syst.)$
$d = 0.2$	$2.62 \pm 0.13(stat.) \pm 0.10(syst.)$
	40–80%
$d = 0.4$	$3.26 \pm 0.15(stat.) \pm 0.13(syst.)$
$d = 0.3$	$3.24 \pm 0.15(stat.) \pm 0.11(syst.)$
$d = 0.2$	$2.99 \pm 0.17(stat.) \pm 0.11(syst.)$

Table 2: Power-law index n extracted from fits of $dR_{\Delta R}/dE_T^{nbr}$ distributions to a power-law function $\propto 1/E_T^n$ for $E_T^{test} > 90$ GeV, for four bins in centrality and three jet radii. The resulting fit error takes into account combined statistical and systematic uncertainties.

bouring jets is suppressed as the centrality of the collision increases.

To further investigate the centrality dependence of neighbouring jet yields, the per-test-jet normalized E_T spectra of neighbouring jets defined in Eq. 2 were evaluated. The resulting differential E_T spectra are shown in Fig. 5 for $d = 0.4$ and $d = 0.2$ jets and three different lower bounds on the test-jet transverse energy, $E_T^{\text{test}} > 80, 90,$ and 110 GeV . The same trend of suppression in central collisions can be seen as that for $R_{\Delta R}$ evaluated as a function of test-jet transverse energy shown in Fig. 4. This is a consequence of the steeply falling shape of the E_T spectra. To better quantify the differences in the E_T spectra of neighbouring jets, the E_T spectra were fitted to a power-law function, $\propto 1/E_T^n$, and the power index was extracted for all three choices of jet radius and four centrality bins. The results are given in Table 2. The E_T spectra measured in central and peripheral collisions differ in the power-law index by approximately two standard deviations for both the $d = 0.4$ and $d = 0.3$ jets, suggesting that the E_T spectra may be less steep in central collisions than in peripheral collisions.

To quantify the centrality dependence of the suppression of neighbouring jets, the ratios $\rho_{R_{\Delta R}}$ were calculated by dividing $R_{\Delta R}$ measured in each centrality bin, except the peripheral bin, by $R_{\Delta R}$ measured in the peripheral (40–80%) bin. Fig. 6 shows $\rho_{R_{\Delta R}}$ evaluated as a function of E_T^{test} and E_T^{nbr} . Some systematic uncertainties cancel in the central-to-peripheral ratio as described in Section 6, resulting in $\rho_{R_{\Delta R}}$ distributions that are dominated by statistical uncertainties. Ratios are evaluated for $d = 0.4$ jets, which suffer the least from the statistical uncertainties, that are still large. Nevertheless, several characteristic features can be observed: the $\rho_{R_{\Delta R}}$ distributions do not exhibit any strong dependence on E_T^{test} ; the suppression factor $\rho_{R_{\Delta R}}$ of the most central collisions is at the level of 0.5–0.7 for all three lower bounds on E_T^{nbr} ; the suppression becomes less pronounced with decreasing centrality. This is qualitatively consistent with the observation of the centrality-dependent suppression of inclusive jet yields [4]. In that measurement, the suppression of the inclusive jet yields was evaluated in terms of the ratio R_{CP} of the inclusive jet yield in central collisions to the yield in 60–80% peripheral collisions spanning the jet p_T range of 40–200 GeV. Values of $R_{\text{CP}} \sim 0.5$ were measured in the 0–10% most central collisions and exhibited only a weak p_T

dependence.

Contrary to a modest dependence of $\rho_{R_{\Delta R}}$ on the test-jet E_T , the $\rho_{R_{\Delta R}}$ evaluated as a function of E_T^{nbr} suggests a decrease of suppression with increasing E_T^{nbr} . Such a decrease in suppression with increasing E_T^{nbr} may in fact be expected. The jet quenching is generally expected to depend on the initial parton energy, but if the splitting happens such that the two partons have similar energy, their quenching would likely be comparable due to similar in-medium path-length travelled by the two partons forming neighbouring jets. Thus, in the configuration of $E_T^{\text{nbr}} \approx E_T^{\text{test}}$ the per-test-jet normalization effectively removes the impact of the suppression.

8. Conclusions

This Letter presents results of a measurement of the production of neighbouring jets using pairs of jets produced at opening angles less than $\pi/2$ in $\eta - \phi$ plane. After subtraction of combinatorial backgrounds from different hard-scattering processes, such jet pairs result from the production of multiple jets in the same hard-scattering process. As such, it is complementary to previous studies of single-jet suppression and dijet asymmetry. By probing the relative quenching of a pair of correlated jets in different collision centralities, this measurement opens up the possibility to study the role of fluctuations in the jet quenching process. This measurement represents a first, exploratory study of how the quark-gluon plasma influences the production and/or later evolution of the neighbouring jets from the same parton shower in heavy-ion collisions.

The jet angular correlations were measured in $\sqrt{s_{\text{NN}}} = 2.76 \text{ TeV Pb+Pb}$ collisions using 0.14 nb^{-1} of data recorded in 2011 by the ATLAS detector at the LHC. The measurements were performed using jets reconstructed with the anti- k_t algorithm for jet radii $d = 0.2, d = 0.3,$ and $d = 0.4$. The production of pairs of correlated jets was quantified using the rate of neighbouring jets that accompany a test jet, $R_{\Delta R}$, evaluated both as a function of test-jet E_T and neighbouring-jet E_T . A significant dependence of $R_{\Delta R}$ on collision centrality is observed in both cases, suggesting a suppression of neighbouring jets which increases with increasing centrality of the collision. The centrality dependence of the suppression was further quantified using the central-to-peripheral ratio of $R_{\Delta R}$ distribu-

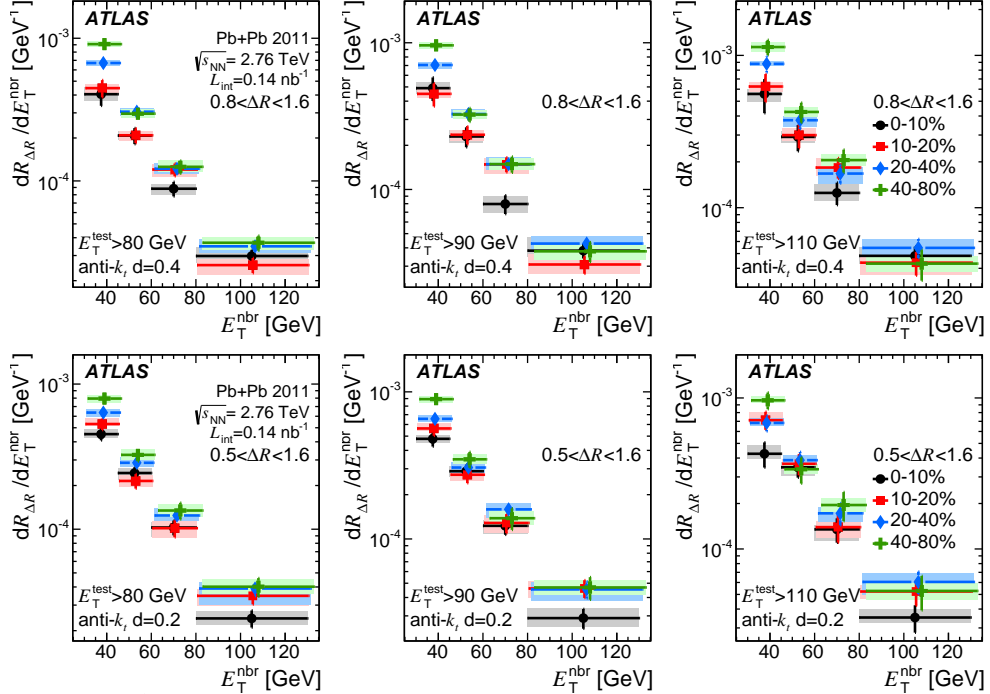


Figure 5: The $dR_{\Delta R}/dE_T^{\text{nbr}}$ distributions for $d = 0.4$ jets (upper) and $d = 0.2$ jets (lower) evaluated as a function of E_T^{nbr} . The three different columns show the $dR_{\Delta R}/dE_T^{\text{nbr}}$ distributions evaluated for three different lower bounds on the test-jet transverse energy, $E_T^{\text{test}} > 80, 90$, and 110 GeV. The four different centrality bins are denoted by different markers in each plot. The shaded bands indicate systematic uncertainties, vertical error bars represent statistical uncertainties. The data points and horizontal uncertainties for 10–20%, 20–40%, and 40–80% centrality bins are shifted along the horizontal axis with respect to 0–10% centrality bin for clarity.

tions, $\rho_{R_{\Delta R}}$. The trends seen in $\rho_{R_{\Delta R}}$ evaluated as a function of neighbouring-jet E_T indicate a decrease in suppression with increasing neighbouring-jet E_T which is, however, of limited significance due to the limited size of the available data sample. The $\rho_{R_{\Delta R}}$ evaluated as a function of test-jet E_T exhibits a suppression reaching values of $0.5 - 0.7$ in 0–10% central collisions and does not show any strong dependence on E_T . This behaviour of the neighbouring jet production can be used to constrain the theoretical models aiming to describe fluctuations in the jet energy loss.

Acknowledgments

We thank CERN for the very successful operation of the LHC, as well as the support staff from our institutions without whom ATLAS could not be operated efficiently.

We acknowledge the support of ANPCyT, Argentina; YerPhI, Armenia; ARC, Australia; BMWFW and FWF, Austria; ANAS, Azerbaijan; SSTC, Belarus; CNPq and FAPESP, Brazil;

NSERC, NRC and CFI, Canada; CERN; CONICYT, Chile; CAS, MOST and NSFC, China; COLCIENCIAS, Colombia; MSMT CR, MPO CR and VSC CR, Czech Republic; DNRF, DNSRC and Lundbeck Foundation, Denmark; EPLANET, ERC and NSRF, European Union; IN2P3-CNRS, CEA-DSM/IRFU, France; GNSF, Georgia; BMBF, DFG, HGF, MPG and AvH Foundation, Germany; GSRT and NSRF, Greece; RGC, Hong Kong SAR, China; ISF, MINERVA, GIF, I-CORE and Benoziyo Center, Israel; INFN, Italy; MEXT and JSPS, Japan; CNRST, Morocco; FOM and NWO, Netherlands; BRF and RCN, Norway; MNiSW and NCN, Poland; GRICES and FCT, Portugal; MNE/IFA, Romania; MES of Russia and NRC KI, Russian Federation; JINR; MSTD, Serbia; MSSR, Slovakia; ARRS and MIZŠ, Slovenia; DST/NRF, South Africa; MINECO, Spain; SRC and Wallenberg Foundation, Sweden; SER, SNSF and Cantons of Bern and Geneva, Switzerland; NSC, Taiwan; TAEK, Turkey; STFC, the Royal Society and Leverhulme Trust, United Kingdom; DOE and NSF, United States of America.

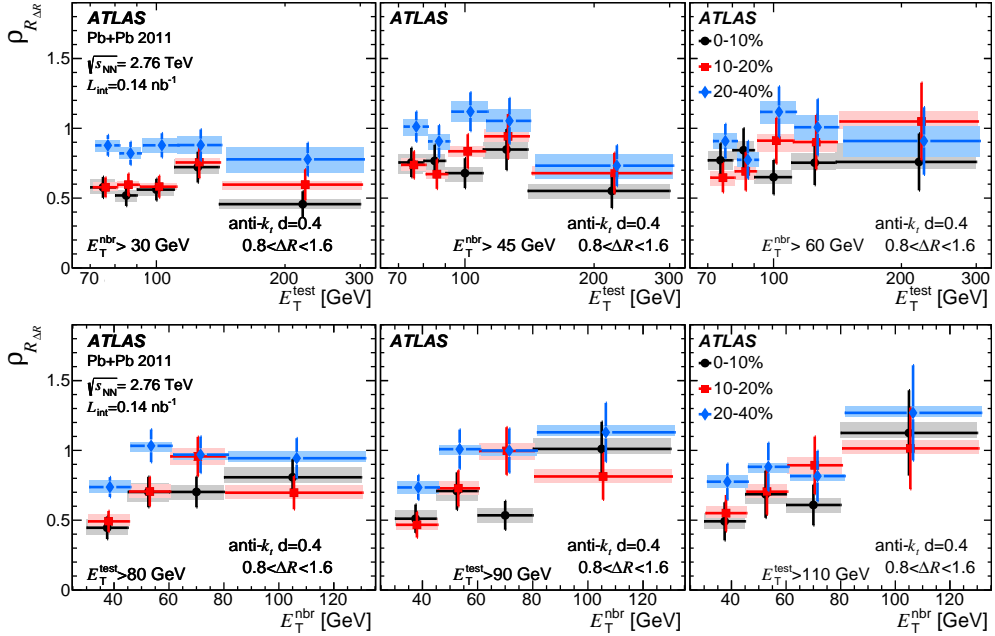


Figure 6: The ratio of $R_{\Delta R}$ for three bins of collision centrality to those in 40–80% collisions, $\rho_{R_{\Delta R}} = R_{\Delta R}|_{\text{cent}}/R_{\Delta R}|_{40-80}$ for $d = 0.4$ jets. The $\rho_{R_{\Delta R}}$ is evaluated as a function of E_T^{test} for three different choices of lower bound on E_T^{nbr} (upper) and as a function of E_T^{nbr} for three different choices of lower bound on E_T^{test} (lower). The shaded bands indicate systematic uncertainties, vertical error bars represent statistical uncertainties. The data points and horizontal uncertainties for 10–20%, 20–40%, and 40–80% centrality bins are shifted along the horizontal axis with respect to 0–10% centrality bin for clarity.

The crucial computing support from all WLCG partners is acknowledged gratefully, in particular from CERN and the ATLAS Tier-1 facilities at TRIUMF (Canada), NDGF (Denmark, Norway, Sweden), CC-IN2P3 (France), KIT/GridKA (Germany), INFN-CNAF (Italy), NL-T1 (Netherlands), PIC (Spain), ASGC (Taiwan), RAL (UK) and BNL (USA) and in the Tier-2 facilities worldwide.

References

- [1] A. Majumder, M. Van Leeuwen, Prog. Part. Nucl. Phys. A66 (2011) 41–92. [arXiv:1002.2206](#).
- [2] ATLAS Collaboration, Phys. Rev. Lett. 105 (2010) 252303. [arXiv:1011.6182](#).
- [3] CMS Collaboration, Phys. Rev. C 84 (2011) 024906. [arXiv:1102.1957](#).
- [4] ATLAS Collaboration, Phys. Lett. B 719 (2013) 220–241. [arXiv:1208.1967](#).
- [5] ATLAS Collaboration, Phys.Rev.Lett. 114 (7) (2015) 072302. [arXiv:1411.2357](#).
- [6] ATLAS Collaboration, Phys. Rev. Lett. 111 (2013) 152301. [arXiv:1306.6469](#).
- [7] V. M. Abazov et al., D0 Collaboration, Phys. Lett. B718 (2012) 56–63. [arXiv:1207.4957](#).
- [8] M. Cacciari, G. P. Salam, G. Soyez, JHEP 04 (2008) 063. [arXiv:0802.1189](#).
- [9] ATLAS Collaboration, JINST 3 (2008) S08003.
- [10] ATLAS Collaboration, JHEP 09 (2010) 056. [arXiv:1005.5254](#).
- [11] ATLAS Collaboration, Phys. Lett. B 707 (2012) 330–348. [arXiv:1108.6018](#).
- [12] T. Sjostrand, S. Mrenna, P. Z. Skands, JHEP 05 (2006) 026. [arXiv:hep-ph/0603175](#).
- [13] ATLAS Collaboration, ATL-PHYS-PUB-2011-009. URL <https://cdsweb.cern.ch/record/1363300>
- [14] S. Agostinelli et al., GEANT4 Collaboration, Nucl. Instrum. Meth. A506 (2003) 250–303.
- [15] ATLAS Collaboration, Eur.Phys.J. C70 (2010) 823–874. [arXiv:1005.4568](#), doi:[10.1140/epjc/s10052-010-1429-9](#).
- [16] ATLAS Collaboration, Eur. Phys. J. C73 (2013) 2304. [arXiv:1112.6426](#).
- [17] ATLAS Collaboration, ATLAS-CONF-2015-016. URL <https://cds.cern.ch/record/2008677>
- [18] I. Lokhtin, A. Snigirev, Eur. Phys. J. C45 (2006) 211–217. [arXiv:hep-ph/0506189](#).
- [19] ATLAS Collaboration, Phys.Lett. B739 (2014) 320–342. [arXiv:1406.2979](#), doi:[10.1016/j.physletb.2014.10.065](#).
- [20] CMS Collaboration, JHEP 10 (2012) 087. [arXiv:1205.5872](#).

The ATLAS Collaboration

G. Aad⁸⁴, B. Abbott¹¹², J. Abdallah¹⁵², S. Abdel Khalek¹¹⁶, O. Abdinov¹¹, R. Aben¹⁰⁶, B. Abi¹¹³, M. Abolins⁸⁹, O.S. AbouZeid¹⁵⁹, H. Abramowicz¹⁵⁴, H. Abreu¹⁵³, R. Abreu³⁰, Y. Abulaiti^{147a,147b}, B.S. Acharya^{165a,165b,a}, L. Adamczyk^{38a}, D.L. Adams²⁵, J. Adelman¹⁷⁷, S. Adomeit⁹⁹, T. Adye¹³⁰, T. Agatonovic-Jovin^{13a}, J.A. Aguilar-Saavedra^{125a,125f}, M. Agustoni¹⁷, S.P. Ahlen²², F. Ahmadov^{64,b}, G. Aielli^{134a,134b}, H. Akerstedt^{147a,147b}, T.P.A. Åkesson⁸⁰, G. Akimoto¹⁵⁶, A.V. Akimov⁹⁵, G.L. Alberghi^{20a,20b}, J. Albert¹⁷⁰, S. Albrand⁵⁵, M.J. Alconada Verzini⁷⁰, M. Aleksi³⁰, I.N. Aleksandrov⁶⁴, C. Alexa^{26a}, G. Alexander¹⁵⁴, G. Alexandre⁴⁹, T. Alexopoulos¹⁰, M. Alhroob^{165a,165c}, G. Alimonti^{90a}, L. Alio⁸⁴, J. Alison³¹, B.M.M. Allbrooke¹⁸, L.J. Allison⁷¹, P.P. Allport⁷³, J. Almond⁸³, A. Aloisio^{103a,103b}, A. Alonso³⁶, F. Alonso⁷⁰, C. Alpigiam⁷⁵, A. Altheimer³⁵, B. Alvarez Gonzalez⁸⁹, M.G. Alviggi^{103a,103b}, K. Amako⁶⁵, Y. Amaral Coutinho^{24a}, C. Amelung²³, D. Amidei⁸⁸, S.P. Amor Dos Santos^{125a,125c}, A. Amorim^{125a,125b}, S. Amoroso⁴⁸, N. Amram¹⁵⁴, G. Amundsen²³, C. Anastopoulos¹⁴⁰, L.S. Ancu⁴⁹, N. Andari³⁰, T. Andeen³⁵, C.F. Anders^{58b}, G. Anders³⁰, K.J. Anderson³¹, A. Andreazza^{90a,90b}, V. Andrei^{58a}, X.S. Anduaga⁷⁰, S. Angelidakis⁹, I. Angelozzi¹⁰⁶, P. Anger⁴⁴, A. Angerami³⁵, F. Anghinolfi³⁰, A.V. Anisenkov^{108,c}, N. Anjos^{125a}, A. Annovi⁴⁷, A. Antonaki⁹, M. Antonelli⁴⁷, A. Antonov⁹⁷, J. Antos^{145b}, F. Anulli^{133a}, M. Aoki⁶⁵, L. Aperio Bella¹⁸, R. Apolle^{119,d}, G. Arabidze⁸⁹, I. Aracena¹⁴⁴, Y. Arai⁶⁵, J.P. Araque^{125a}, A.T.H. Arce⁴⁵, J-F. Arguin⁹⁴, S. Argyropoulos⁴², M. Arik^{19a}, A.J. Armbruster³⁰, O. Arnaez³⁰, V. Arnal⁸¹, H. Arnold⁴⁸, M. Arratia²⁸, O. Arslan²¹, A. Artamonov⁹⁶, G. Artoni²³, S. Asai¹⁵⁶, N. Asbah⁴², A. Ashkenazi¹⁵⁴, B. Åsman^{147a,147b}, L. Asquith⁶, K. Assamagan²⁵, R. Astalos^{145a}, M. Atkinson¹⁶⁶, N.B. Atlay¹⁴², B. Auerbach⁶, K. Augsten¹²⁷, M. Aurousseau^{146b}, G. Avolio³⁰, G. Azuelos^{94,e}, Y. Azuma¹⁵⁶, M.A. Baak³⁰, A.E. Baas^{58a}, C. Bacci^{135a,135b}, H. Bachacou¹³⁷, K. Bachas¹⁵⁵, M. Backes³⁰, M. Backhaus³⁰, J. Backus Mayes¹⁴⁴, E. Badescu^{26a}, P. Bagiacchi^{133a,133b}, P. Bagnaia^{133a,133b}, Y. Bai^{33a}, T. Bain³⁵, J.T. Baines¹³⁰, O.K. Baker¹⁷⁷, P. Balek¹²⁸, F. Balli¹³⁷, E. Banas³⁹, Sw. Banerjee¹⁷⁴, A.A.E. Bannoura¹⁷⁶, V. Bansal¹⁷⁰, H.S. Bansil¹⁸, L. Barak¹⁷³, E.L. Barberio⁸⁷, D. Barberis^{50a,50b}, M. Barbero⁸⁴, T. Barillari¹⁰⁰, M. Barisonzi¹⁷⁶, T. Barklow¹⁴⁴, N. Barlow²⁸, B.M. Barnett¹³⁰, R.M. Barnett¹⁵, Z. Barnovska⁵, A. Baroncelli^{135a}, G. Barone⁴⁹, A.J. Barr¹¹⁹, F. Barreiro⁸¹, J. Barreiro Guimarães da Costa⁵⁷, R. Bartoldus¹⁴⁴, A.E. Barton⁷¹, P. Bartos^{145a}, V. Bartsch¹⁵⁰, A. Bassalat¹¹⁶, A. Basye¹⁶⁶, R.L. Bates⁵³, J.R. Batley²⁸, M. Battaglia¹³⁸, M. Battistin³⁰, F. Bauer¹³⁷, H.S. Bawa^{144,f}, M.D. Beattie⁷¹, T. Beau⁷⁹, P.H. Beauchemin¹⁶², R. Beccherle^{123a,123b}, P. Bechtle²¹, H.P. Beck^{17,g}, K. Becker¹⁷⁶, S. Becker⁹⁹, M. Beckingham¹⁷¹, C. Becot¹¹⁶, A.J. Beddall^{19c}, A. Beddall^{19c}, S. Bedikian¹⁷⁷, V.A. Bednyakov⁶⁴, C.P. Bee¹⁴⁹, L.J. Beemster¹⁰⁶, T.A. Beermann¹⁷⁶, M. Begel²⁵, J.K. Behr¹¹⁹, C. Belanger-Champagne⁸⁶, P.J. Bell⁴⁹, W.H. Bell⁴⁹, G. Bella¹⁵⁴, L. Bellagamba^{20a}, A. Bellerive²⁹, M. Bellomo⁸⁵, K. Belotskiy⁹⁷, O. Beltramo³⁰, O. Benary¹⁵⁴, D. Benchekroun^{136a}, K. Bendtz^{147a,147b}, N. Benekos¹⁶⁶, Y. Benhammou¹⁵⁴, E. Benhar Noccioli⁴⁹, J.A. Benitez Garcia^{160b}, D.P. Benjamin⁴⁵, J.R. Bensinger²³, K. Benslama¹³¹, S. Bentvelsen¹⁰⁶, D. Berge¹⁰⁶, E. Bergeaas Kuutmann¹⁶⁷, N. Berger⁵, F. Berghaus¹⁷⁰, J. Beringer¹⁵, C. Bernard²², P. Bernat⁷⁷, C. Bernius⁷⁸, F.U. Bernlochner¹⁷⁰, T. Berry⁷⁶, P. Berta¹²⁸, C. Bertella⁸⁴, G. Bertoli^{147a,147b}, F. Bertolucci^{123a,123b}, C. Bertsche¹¹², D. Bertsche¹¹², M.I. Besana^{90a}, G.J. Besjes¹⁰⁵, O. Bessidskaia Bylund^{147a,147b}, M. Bessner⁴², N. Besson¹³⁷, C. Betancourt⁴⁸, S. Bethke¹⁰⁰, W. Bhimji⁴⁶, R.M. Bianchi¹²⁴, L. Bianchini²³, M. Bianco³⁰, O. Biebel⁹⁹, S.P. Bieniek⁷⁷, K. Bierwagen⁵⁴, J. Biesiada¹⁵, M. Biglietti^{135a}, J. Bilbao De Mendizabal⁴⁹, H. Bilokon⁴⁷, M. Bindi⁵⁴, S. Binet¹¹⁶, A. Bingul^{19c}, C. Bini^{133a,133b}, C.W. Black¹⁵¹, J.E. Black¹⁴⁴, K.M. Black²², D. Blackburn¹³⁹, R.E. Blair⁶, J.-B. Blanchard¹³⁷, T. Blazek^{145a}, I. Bloch⁴², C. Blocker²³, W. Blum^{82,*}, U. Blumenschein⁵⁴, G.J. Bobbink¹⁰⁶, V.S. Bobrovnikov^{108,c}, S.S. Bocchetta⁸⁰, A. Bocci⁴⁵, C. Bock⁹⁹, C.R. Boddy¹¹⁹, M. Boehler⁴⁸, T.T. Boek¹⁷⁶, J.A. Bogaerts³⁰, A.G. Bogdanchikov¹⁰⁸, A. Bogouch^{91,*}, C. Bohm^{147a}, J. Bohm¹²⁶, V. Boisvert⁷⁶, T. Bold^{38a}, V. Boldea^{26a}, A.S. Boldyrev⁹⁸, M. Bomben⁷⁹, M. Bona⁷⁵, M. Boonekamp¹³⁷, A. Borisov¹²⁹, G. Borissov⁷¹, M. Borri⁸³, S. Borroni⁴², J. Bortfeldt⁹⁹, V. Bortolotto^{135a,135b}, K. Bos¹⁰⁶, D. Boscherini^{20a}, M. Bosman¹², H. Boterenbrood¹⁰⁶, J. Boudreau¹²⁴, J. Bouffard², E.V. Bouhova-Thacker⁷¹, D. Boumediene³⁴, C. Bourdarios¹¹⁶, N. Bousson¹¹³, S. Boutouil^{136d}, A. Boveia³¹, J. Boyd³⁰, I.R. Boyko⁶⁴, J. Bracinik¹⁸, A. Brandt⁸, G. Brandt¹⁵, O. Brandt^{58a}, U. Bratzler¹⁵⁷, B. Brau⁸⁵, J.E. Brau¹¹⁵, H.M. Braun^{176,*}, S.F. Brazzale^{165a,165c},

B. Brelier¹⁵⁹, K. Brendlinger¹²¹, A.J. Brennan⁸⁷, R. Brenner¹⁶⁷, S. Bressler¹⁷³, K. Bristow^{146c},
 T.M. Bristow⁴⁶, D. Britton⁵³, F.M. Brochu²⁸, I. Brock²¹, R. Brock⁸⁹, C. Bromberg⁸⁹, J. Bronner¹⁰⁰,
 G. Brooijmans³⁵, T. Brooks⁷⁶, W.K. Brooks^{32b}, J. Brosamer¹⁵, E. Brost¹¹⁵, J. Brown⁵⁵,
 P.A. Bruckman de Renstrom³⁹, D. Bruncko^{145b}, R. Bruneliere⁴⁸, S. Brunet⁶⁰, A. Bruni^{20a}, G. Bruni^{20a},
 M. Bruschi^{20a}, L. Bryngemark⁸⁰, T. Buanes¹⁴, Q. Buat¹⁴³, F. Bucci⁴⁹, P. Buchholz¹⁴²,
 R.M. Buckingham¹¹⁹, A.G. Buckley⁵³, S.I. Buda^{26a}, I.A. Budagov⁶⁴, F. Buehrer⁴⁸, L. Bugge¹¹⁸,
 M.K. Bugge¹¹⁸, O. Bulekov⁹⁷, A.C. Bundock⁷³, H. Burckhart³⁰, S. Burdin⁷³, B. Burghgrave¹⁰⁷,
 S. Burke¹³⁰, I. Burmeister⁴³, E. Busato³⁴, D. Büscher⁴⁸, V. Büscher⁸², P. Bussey⁵³, C.P. Buszello¹⁶⁷,
 B. Butler⁵⁷, J.M. Butler²², A.I. Butt³, C.M. Buttar⁵³, J.M. Butterworth⁷⁷, P. Butti¹⁰⁶, W. Buttinger²⁸,
 A. Buzatu⁵³, M. Byszewski¹⁰, S. Cabrera Urbán¹⁶⁸, D. Caforio^{20a,20b}, O. Cakir^{4a}, P. Calafiura¹⁵,
 A. Calandri¹³⁷, G. Calderini⁷⁹, P. Calfayan⁹⁹, R. Calkins¹⁰⁷, L.P. Caloba^{24a}, D. Calvet³⁴, S. Calvet³⁴,
 R. Camacho Toro⁴⁹, S. Camarda⁴², D. Cameron¹¹⁸, L.M. Caminada¹⁵, R. Caminal Armadans¹²,
 S. Campana³⁰, M. Campanelli⁷⁷, A. Campoverde¹⁴⁹, V. Canale^{103a,103b}, A. Canepa^{160a}, M. Cano Bret⁷⁵,
 J. Cantero⁸¹, R. Cantrill^{125a}, T. Cao⁴⁰, M.D.M. Capeans Garrido³⁰, I. Caprini^{26a}, M. Caprini^{26a},
 M. Capua^{37a,37b}, R. Caputo⁸², R. Cardarelli^{134a}, T. Carli³⁰, G. Carlino^{103a}, L. Carminati^{90a,90b},
 S. Caron¹⁰⁵, E. Carquin^{32a}, G.D. Carrillo-Montoya^{146c}, J.R. Carter²⁸, J. Carvalho^{125a,125c}, D. Casadei⁷⁷,
 M.P. Casado¹², M. Casolino¹², E. Castaneda-Miranda^{146b}, A. Castelli¹⁰⁶, V. Castillo Gimenez¹⁶⁸,
 N.F. Castro^{125a,h}, P. Catastini⁵⁷, A. Catinaccio³⁰, J.R. Catmore¹¹⁸, A. Cattai³⁰, G. Cattani^{134a,134b},
 J. Caudron⁸², S. Caughron⁸⁹, V. Cavaliere¹⁶⁶, D. Cavalli^{90a}, M. Cavalli-Sforza¹², V. Cavasinni^{123a,123b},
 F. Ceradini^{135a,135b}, B.C. Cerio⁴⁵, K. Cerny¹²⁸, A.S. Cerqueira^{24b}, A. Cerri¹⁵⁰, L. Cerrito⁷⁵, F. Cerutti¹⁵,
 M. Cerv³⁰, A. Cervelli¹⁷, S.A. Cetin^{19b}, A. Chafaq^{136a}, D. Chakraborty¹⁰⁷, I. Chalupkova¹²⁸, P. Chang¹⁶⁶,
 B. Chapleau⁸⁶, J.D. Chapman²⁸, D. Charfeddine¹¹⁶, D.G. Charlton¹⁸, C.C. Chau¹⁵⁹,
 C.A. Chavez Barajas¹⁵⁰, S. Cheatham⁸⁶, A. Chegwidden⁸⁹, S. Chekanov⁶, S.V. Chekulaev^{160a},
 G.A. Chelkov^{64,i}, M.A. Chelstowska⁸⁸, C. Chen⁶³, H. Chen²⁵, K. Chen¹⁴⁹, L. Chen^{33d,j}, S. Chen^{33c},
 X. Chen^{146c}, Y. Chen⁶⁶, Y. Chen³⁵, H.C. Cheng⁸⁸, Y. Cheng³¹, A. Cheplakov⁶⁴,
 R. Cherkaoui El Moursli^{136e}, V. Chernyatin^{25,*}, E. Cheu⁷, L. Chevalier¹³⁷, V. Chiarella⁴⁷,
 G. Chiefari^{103a,103b}, J.T. Childers⁶, A. Chilingarov⁷¹, G. Chiodini^{72a}, A.S. Chisholm¹⁸, R.T. Chislett⁷⁷,
 A. Chitan^{26a}, M.V. Chizhov⁶⁴, S. Chouridou⁹, B.K.B. Chow⁹⁹, D. Chromek-Burckhart³⁰, M.L. Chu¹⁵²,
 J. Chudoba¹²⁶, J.J. Chwastowski³⁹, L. Chytka¹¹⁴, G. Ciapetti^{133a,133b}, A.K. Ciftci^{4a}, R. Ciftci^{4a},
 D. Cinca⁵³, V. Cindro⁷⁴, A. Ciocio¹⁵, P. Cirkovic¹³, Z.H. Citron¹⁷³, M. Ciubancan^{26a}, A. Clark⁴⁹,
 P.J. Clark⁴⁶, R.N. Clarke¹⁵, W. Cleland¹²⁴, J.C. Clemens⁸⁴, C. Clement^{147a,147b}, Y. Coadou⁸⁴,
 M. Cobal^{165a,165c}, A. Coccaro¹³⁹, J. Cochran⁶³, L. Coffey²³, J.G. Cogan¹⁴⁴, J. Coggeshall¹⁶⁶, B. Cole³⁵,
 S. Cole¹⁰⁷, A.P. Colijn¹⁰⁶, J. Collot⁵⁵, T. Colombo^{58c}, G. Colon⁸⁵, G. Compostella¹⁰⁰,
 P. Conde Muñoz^{125a,125b}, E. Coniavitis⁴⁸, M.C. Conidi¹², S.H. Connell^{146b}, I.A. Connelly⁷⁶,
 S.M. Consonni^{90a,90b}, V. Consorti⁴⁸, S. Constantinescu^{26a}, C. Conta^{120a,120b}, G. Conti⁵⁷, F. Conventi^{103a,k},
 M. Cooke¹⁵, B.D. Cooper⁷⁷, A.M. Cooper-Sarkar¹¹⁹, N.J. Cooper-Smith⁷⁶, K. Copic¹⁵, T. Cornelissen¹⁷⁶,
 M. Corradi^{20a}, F. Corriveau^{86,l}, A. Corso-Radu¹⁶⁴, A. Cortes-Gonzalez¹², G. Cortiana¹⁰⁰, G. Costa^{90a},
 M.J. Costa¹⁶⁸, D. Costanzo¹⁴⁰, D. Côté⁸, G. Cottin²⁸, G. Cowan⁷⁶, B.E. Cox⁸³, K. Cranmer¹⁰⁹, G. Cree²⁹,
 S. Crépé-Renaudin⁵⁵, F. Crescioli⁷⁹, W.A. Cribbs^{147a,147b}, M. Crispin Ortuzar¹¹⁹, M. Cristinziani²¹,
 V. Croft¹⁰⁵, G. Crosetti^{37a,37b}, C.-M. Cuciuc^{26a}, T. Cuhadar Donszelmann¹⁴⁰, J. Cummings¹⁷⁷,
 M. Curatolo⁴⁷, C. Cuthbert¹⁵¹, H. Czirr¹⁴², P. Czodrowski³, Z. Czyczula¹⁷⁷, S. D'Auria⁵³, M. D'Onofrio⁷³,
 M.J. Da Cunha Sargedas De Sousa^{125a,125b}, C. Da Via⁸³, W. Dabrowski^{38a}, A. Dafinca¹¹⁹, T. Dai⁸⁸,
 O. Dale¹⁴, F. Dallaire⁹⁴, C. Dallapiccola⁸⁵, M. Dam³⁶, A.C. Daniells¹⁸, M. Dano Hoffmann¹³⁷, V. Dao⁴⁸,
 G. Darbo^{50a}, S. Darmora⁸, J. Dassoulas⁴², A. DattaGupta⁶⁰, W. Davey²¹, C. David¹⁷⁰, T. Davidek¹²⁸,
 E. Davies^{119,d}, M. Davies¹⁵⁴, O. Davignon⁷⁹, A.R. Davison⁷⁷, P. Davison⁷⁷, Y. Davygora^{58a}, E. Dawe¹⁴³,
 I. Dawson¹⁴⁰, R.K. Daya-Ishmukhametova⁸⁵, K. De⁸, R. de Asmundis^{103a}, S. De Castro^{20a,20b},
 S. De Cecco⁷⁹, N. De Groot¹⁰⁵, P. de Jong¹⁰⁶, H. De la Torre⁸¹, F. De Lorenzi⁶³, L. De Nooij¹⁰⁶,
 D. De Pedis^{133a}, A. De Salvo^{133a}, U. De Sanctis^{165a,165b}, A. De Santo¹⁵⁰, J.B. De Vivie De Regie¹¹⁶,
 W.J. Dearnaley⁷¹, R. Debbe²⁵, C. Debenedetti¹³⁸, B. Dechenaux⁵⁵, D.V. Dedovich⁶⁴, I. Deigaard¹⁰⁶,
 J. Del Peso⁸¹, T. Del Prete^{123a,123b}, F. Deliot¹³⁷, C.M. Delitzsch⁴⁹, M. Deliyergiyev⁷⁴, A. Dell'Acqua³⁰,
 L. Dell'Asta²², M. Dell'Orso^{123a,123b}, M. Della Pietra^{103a,k}, D. della Volpe⁴⁹, M. Delmastro⁵,
 P.A. Delsart⁵⁵, C. Deluca¹⁰⁶, S. Demers¹⁷⁷, M. Demichev⁶⁴, A. Demilly⁷⁹, S.P. Denisov¹²⁹,

D. Derendarz³⁹, J.E. Derkaoui^{136d}, F. Derue⁷⁹, P. Dervan⁷³, K. Desch²¹, C. Deterre⁴², P.O. Deviveiros¹⁰⁶, A. Dewhurst¹³⁰, S. Dhaliwal¹⁰⁶, A. Di Ciaccio^{134a,134b}, L. Di Ciaccio⁵, A. Di Domenico^{133a,133b}, C. Di Donato^{103a,103b}, A. Di Girolamo³⁰, B. Di Girolamo³⁰, A. Di Mattia¹⁵³, B. Di Micco^{135a,135b}, R. Di Nardo⁴⁷, A. Di Simone⁴⁸, R. Di Sipio^{20a,20b}, D. Di Valentino²⁹, F.A. Dias⁴⁶, M.A. Diaz^{32a}, E.B. Diehl⁸⁸, J. Dietrich⁴², T.A. Dietzsch^{58a}, S. Diglio⁸⁴, A. Dimitrievska^{13a}, J. Dingfelder²¹, C. Dionisi^{133a,133b}, P. Dita^{26a}, S. Dita^{26a}, F. Dittus³⁰, F. Djama⁸⁴, T. Djobava^{51b}, J.I. Djuvslund^{58a}, M.A.B. do Vale^{24c}, A. Do Valle Wemans^{125a,125g}, T.K.O. Doan⁵, D. Dobos³⁰, C. Doglioni⁴⁹, T. Doherty⁵³, T. Dohmae¹⁵⁶, J. Dolejsi¹²⁸, Z. Dolezal¹²⁸, B.A. Dolgoshein^{97,*}, M. Donadelli^{24d}, S. Donati^{123a,123b}, P. Dondero^{120a,120b}, J. Donini³⁴, J. Dopke¹³⁰, A. Doria^{103a}, M.T. Dova⁷⁰, A.T. Doyle⁵³, M. Dris¹⁰, J. Dubbert⁸⁸, S. Dube¹⁵, E. Dubreuil³⁴, E. Duchovni¹⁷³, G. Duckeck⁹⁹, O.A. Ducu^{26a}, D. Duda¹⁷⁶, A. Dudarev³⁰, F. Dudziak⁶³, L. Duflot¹¹⁶, L. Duguid⁷⁶, M. Dührssen³⁰, M. Dunford^{58a}, H. Duran Yildiz^{4a}, M. Düren⁵², A. Durglishvili^{51b}, M. Dwuznik^{38a}, M. Dyndal^{38a}, J. Ebke⁹⁹, W. Edson², N.C. Edwards⁴⁶, W. Ehrenfeld²¹, T. Eifert¹⁴⁴, G. Eigen¹⁴, K. Einsweiler¹⁵, T. Ekelof¹⁶⁷, M. El Kacimi^{136c}, M. Ellert¹⁶⁷, S. Elles⁵, F. Ellinghaus⁸², N. Ellis³⁰, J. Elmsheuser⁹⁹, M. Elsing³⁰, D. Emeliyanov¹³⁰, Y. Enari¹⁵⁶, O.C. Endner⁸², M. Endo¹¹⁷, J. Erdmann¹⁷⁷, A. Ereditato¹⁷, D. Eriksson^{147a}, G. Ernis¹⁷⁶, J. Ernst², M. Ernst²⁵, J. Ernwein¹³⁷, D. Errede¹⁶⁶, S. Errede¹⁶⁶, E. Ertel⁸², M. Escalier¹¹⁶, H. Esch⁴³, C. Escobar¹²⁴, B. Esposito⁴⁷, A.I. Etievre¹³⁷, E. Etzion¹⁵⁴, H. Evans⁶⁰, A. Ezhilov¹²², L. Fabbri^{20a,20b}, G. Facini³¹, R.M. Fakhrutdinov¹²⁹, S. Falciano^{133a}, R.J. Falla⁷⁷, J. Faltova¹²⁸, Y. Fang^{33a}, M. Fanti^{90a,90b}, A. Farbin⁸, A. Farilla^{135a}, T. Farooque¹², S. Farrell¹⁵, S.M. Farrington¹⁷¹, P. Farthouat³⁰, F. Fassi^{136e}, P. Fassnacht³⁰, D. Fassouliotis⁹, A. Favareto^{50a,50b}, L. Fayard¹¹⁶, P. Federic^{145a}, O.L. Fedin^{122,m}, W. Fedorko¹⁶⁹, M. Fehling-Kaschek⁴⁸, S. Feigl³⁰, L. Feligioni⁸⁴, C. Feng^{33d}, E.J. Feng⁶, H. Feng⁸⁸, A.B. Fenyuk¹²⁹, S. Fernandez Perez³⁰, S. Ferrag⁵³, J. Ferrando⁵³, A. Ferrari¹⁶⁷, P. Ferrari¹⁰⁶, R. Ferrari^{120a}, D.E. Ferreira de Lima⁵³, A. Ferrer¹⁶⁸, D. Ferrere⁴⁹, C. Ferretti⁸⁸, A. Ferretto Parodi^{50a,50b}, M. Fiascaris³¹, F. Fiedler⁸², A. Filipčič⁷⁴, M. Filipuzzi⁴², F. Filthaut¹⁰⁵, M. Fincke-Keeler¹⁷⁰, K.D. Finelli¹⁵¹, M.C.N. Fiolhais^{125a,125c}, L. Fiorini¹⁶⁸, A. Firan⁴⁰, A. Fischer², J. Fischer¹⁷⁶, W.C. Fisher⁸⁹, E.A. Fitzgerald²³, M. Flechl⁴⁸, I. Fleck¹⁴², P. Fleischmann⁸⁸, S. Fleischmann¹⁷⁶, G.T. Fletcher¹⁴⁰, G. Fletcher⁷⁵, T. Flick¹⁷⁶, A. Floderus⁸⁰, L.R. Flores Castillo^{174,n}, A.C. Florez Bustos^{160b}, M.J. Flowerdew¹⁰⁰, A. Formica¹³⁷, A. Forti⁸³, D. Fortin^{160a}, D. Fournier¹¹⁶, H. Fox⁷¹, S. Fracchia¹², P. Francavilla⁷⁹, M. Franchini^{20a,20b}, S. Franchino³⁰, D. Francis³⁰, L. Franconi¹¹⁸, M. Franklin⁵⁷, S. Franz⁶¹, M. Fraternali^{120a,120b}, S.T. French²⁸, C. Friedrich⁴², F. Friedrich⁴⁴, D. Froidevaux³⁰, J.A. Frost²⁸, C. Fukunaga¹⁵⁷, E. Fullana Torregrosa⁸², B.G. Fulsom¹⁴⁴, J. Fuster¹⁶⁸, C. Gabaldon⁵⁵, O. Gabizon¹⁷³, A. Gabrielli^{20a,20b}, A. Gabrielli^{133a,133b}, S. Gadatsch¹⁰⁶, S. Gadomski⁴⁹, G. Gagliardi^{50a,50b}, P. Gagnon⁶⁰, C. Galea¹⁰⁵, B. Galhardo^{125a,125c}, E.J. Gallas¹¹⁹, V. Gallo¹⁷, B.J. Gallop¹³⁰, P. Gallus¹²⁷, G. Galster³⁶, K.K. Gan¹¹⁰, R.P. Gandrajula⁶², J. Gao^{33b,84}, Y.S. Gao^{144,f}, F.M. Garay Walls⁴⁶, F. Garberson¹⁷⁷, C. García¹⁶⁸, J.E. García Navarro¹⁶⁸, M. Garcia-Sciveres¹⁵, R.W. Gardner³¹, N. Garelli¹⁴⁴, V. Garonne³⁰, C. Gatti⁴⁷, G. Gaudio^{120a}, B. Gaur¹⁴², L. Gauthier⁹⁴, P. Gauzzi^{133a,133b}, I.L. Gavrilenko⁹⁵, C. Gay¹⁶⁹, G. Gaycken²¹, E.N. Gazis¹⁰, P. Ge^{33d}, Z. Gecse¹⁶⁹, C.N.P. Gee¹³⁰, D.A.A. Geerts¹⁰⁶, Ch. Geich-Gimbel²¹, C. Gemme^{50a}, A. Gemmell⁵³, M.H. Genest⁵⁵, S. Gentile^{133a,133b}, M. George⁵⁴, S. George⁷⁶, D. Gerbaudo¹⁶⁴, A. Gershon¹⁵⁴, H. Ghazlane^{136b}, N. Ghodbane³⁴, B. Giacobbe^{20a}, S. Giagu^{133a,133b}, V. Giangiobbe¹², P. Giannetti^{123a,123b}, F. Gianotti³⁰, B. Gibbard²⁵, S.M. Gibson⁷⁶, M. Gilchriesse¹⁵, T.P.S. Gillam²⁸, D. Gillberg³⁰, G. Gilles³⁴, D.M. Gingrich^{3,e}, N. Giokaris⁹, M.P. Giordani^{165a,165c}, R. Giordano^{103a,103b}, F.M. Giorgi^{20a}, F.M. Giorgi¹⁶, P.F. Giraud¹³⁷, D. Giugni^{90a}, C. Giuliani⁴⁸, M. Giulini^{58b}, B.K. Gjelsten¹¹⁸, S. Gkaitatzis¹⁵⁵, I. Gkalias¹⁵⁵, L.K. Gladilin⁹⁸, C. Glasman⁸¹, J. Glatzer³⁰, P.C.F. Glaysher⁴⁶, A. Glazov⁴², G.L. Glonti⁶⁴, M. Goblirsch-Kolb¹⁰⁰, J.R. Goddard⁷⁵, J. Godfrey¹⁴³, J. Godlewski³⁰, C. Goeringer⁸², S. Goldfarb⁸⁸, T. Golling¹⁷⁷, D. Golubkov¹²⁹, A. Gomes^{125a,125b,125d}, L.S. Gomez Fajardo⁴², R. Gonçalo^{125a}, J. Goncalves Pinto Firmino Da Costa¹³⁷, L. Gonella²¹, S. González de la Hoz¹⁶⁸, G. Gonzalez Parra¹², S. Gonzalez-Sevilla⁴⁹, L. Goossens³⁰, P.A. Gorbounov⁹⁶, H.A. Gordon²⁵, I. Gorelov¹⁰⁴, B. Gorini³⁰, E. Gorini^{72a,72b}, A. Gorišek⁷⁴, E. Gornicki³⁹, A.T. Goshaw⁶, C. Gössling⁴³, M.I. Gostkin⁶⁴, M. Gouighri^{136a}, D. Goujdami^{136c}, M.P. Goulette⁴⁹, A.G. Goussiou¹³⁹, C. Goy⁵, S. Gozpinar²³, H.M.X. Grabas¹³⁷, L. Graber⁵⁴, I. Grabowska-Bold^{38a}, P. Grafström^{20a,20b}, K.-J. Grahn⁴², J. Gramling⁴⁹, E. Gramstad¹¹⁸, S. Grancagnolo¹⁶, V. Grassi¹⁴⁹, V. Gratchev¹²²,

H.M. Gray³⁰, E. Graziani^{135a}, O.G. Grebenyuk¹²², Z.D. Greenwood^{78,o}, K. Gregersen⁷⁷, I.M. Gregor⁴², P. Grenier¹⁴⁴, J. Griffiths⁸, A.A. Grillo¹³⁸, K. Grimm⁷¹, S. Grinstein^{12,p}, Ph. Gris³⁴, Y.V. Grishkevich⁹⁸, J.-F. Grivaz¹¹⁶, J.P. Grohs⁴⁴, A. Grohsjean⁴², E. Gross¹⁷³, J. Grosse-Knetter⁵⁴, G.C. Grossi^{134a,134b}, J. Groth-Jensen¹⁷³, Z.J. Grout¹⁵⁰, L. Guan^{33b}, J. Guenther¹²⁷, F. Guescini⁴⁹, D. Guest¹⁷⁷, O. Gueta¹⁵⁴, C. Guicheney³⁴, E. Guido^{50a,50b}, T. Guillemin¹¹⁶, S. Guindon², U. Gul⁵³, C. Gumpert⁴⁴, J. Guo³⁵, S. Gupta¹¹⁹, P. Gutierrez¹¹², N.G. Gutierrez Ortiz⁵³, C. Gutschow⁷⁷, N. Guttman¹⁵⁴, C. Guyot¹³⁷, C. Gwenlan¹¹⁹, C.B. Gwilliam⁷³, A. Haas¹⁰⁹, C. Haber¹⁵, H.K. Hadavand⁸, N. Haddad^{136e}, P. Haefner²¹, S. Hageböck²¹, Z. Hajduk³⁹, H. Hakobyan¹⁷⁸, M. Haleem⁴², D. Hall¹¹⁹, G. Halladjian⁸⁹, K. Hamacher¹⁷⁶, P. Hamal¹¹⁴, K. Hamano¹⁷⁰, M. Hamer⁵⁴, A. Hamilton^{146a}, S. Hamilton¹⁶², G.N. Hamity^{146c}, P.G. Hamnett⁴², L. Han^{33b}, K. Hanagaki¹¹⁷, K. Hanawa¹⁵⁶, M. Hance¹⁵, P. Hanke^{58a}, R. Hanna¹³⁷, J.B. Hansen³⁶, J.D. Hansen³⁶, P.H. Hansen³⁶, K. Hara¹⁶¹, A.S. Hard¹⁷⁴, T. Harenberg¹⁷⁶, F. Hariri¹¹⁶, S. Harkusha⁹¹, D. Harper⁸⁸, R.D. Harrington⁴⁶, O.M. Harris¹³⁹, P.F. Harrison¹⁷¹, F. Hartjes¹⁰⁶, M. Hasegawa⁶⁶, S. Hasegawa¹⁰², Y. Hasegawa¹⁴¹, A. Hasib¹¹², S. Hassani¹³⁷, S. Haug¹⁷, M. Hauschild³⁰, R. Hauser⁸⁹, M. Havranek¹²⁶, C.M. Hawkes¹⁸, R.J. Hawkings³⁰, A.D. Hawkins⁸⁰, T. Hayashi¹⁶¹, D. Hayden⁸⁹, C.P. Hays¹¹⁹, H.S. Hayward⁷³, S.J. Haywood¹³⁰, S.J. Head¹⁸, T. Heck⁸², V. Hedberg⁸⁰, L. Heelan⁸, S. Heim¹²¹, T. Heim¹⁷⁶, B. Heinemann¹⁵, L. Heinrich¹⁰⁹, J. Hejbal¹²⁶, L. Helary²², C. Heller⁹⁹, M. Heller³⁰, S. Hellman^{147a,147b}, D. Hellmich²¹, C. Helsens³⁰, J. Henderson¹¹⁹, R.C.W. Henderson⁷¹, Y. Heng¹⁷⁴, C. Henglert⁴², A. Henrichs¹⁷⁷, A.M. Henriques Correia³⁰, S. Henrot-Versille¹¹⁶, C. Hensel⁵⁴, G.H. Herbert¹⁶, Y. Hernández Jiménez¹⁶⁸, R. Herrberg-Schubert¹⁶, G. Herten⁴⁸, R. Hertenberger⁹⁹, L. Hervas³⁰, G.G. Hesketh⁷⁷, N.P. Hessey¹⁰⁶, R. Hickling⁷⁵, E. Higón-Rodriguez¹⁶⁸, E. Hill¹⁷⁰, J.C. Hill²⁸, K.H. Hiller⁴², S. Hillert²¹, S.J. Hillier¹⁸, I. Hinchliffe¹⁵, E. Hines¹²¹, M. Hirose¹⁵⁸, D. Hirschbuehl¹⁷⁶, J. Hobbs¹⁴⁹, N. Hod¹⁰⁶, M.C. Hodgkinson¹⁴⁰, P. Hodgson¹⁴⁰, A. Hoecker³⁰, M.R. Hoeferkamp¹⁰⁴, F. Hoenig⁹⁹, J. Hoffman⁴⁰, D. Hoffmann⁸⁴, M. Hohlfeld⁸², T.R. Holmes¹⁵, T.M. Hong¹²¹, L. Hooft van Huysduynen¹⁰⁹, J-Y. Hostachy⁵⁵, S. Hou¹⁵², A. Hoummada^{136a}, J. Howard¹¹⁹, J. Howarth⁴², M. Hrabovsky¹¹⁴, I. Hristova¹⁶, J. Hrvnac¹¹⁶, T. Hrynn'ova⁵, C. Hsu^{146c}, P.J. Hsu⁸², S.-C. Hsu¹³⁹, D. Hu³⁵, X. Hu⁸⁸, Y. Huang⁴², Z. Hubacek³⁰, F. Hubaut⁸⁴, F. Huegging²¹, T.B. Huffman¹¹⁹, E.W. Hughes³⁵, G. Hughes⁷¹, M. Huhtinen³⁰, T.A. Hülsing⁸², M. Hurwitz¹⁵, N. Huseynov^{64,b}, J. Huston⁸⁹, J. Huth⁵⁷, G. Iacobucci⁴⁹, G. Iakovidis¹⁰, I. Ibragimov¹⁴², L. Iconomidou-Fayard¹¹⁶, E. Ideal¹⁷⁷, P. Iengo^{103a}, O. Igonkina¹⁰⁶, T. Iizawa¹⁷², Y. Ikegami⁶⁵, K. Ikematsu¹⁴², M. Ikeno⁶⁵, Y. Ilchenko^{31,q}, D. Iliadis¹⁵⁵, N. Ilic¹⁵⁹, Y. Inamaru⁶⁶, T. Ince¹⁰⁰, P. Ioannou⁹, M. Iodice^{135a}, K. Iordanidou⁹, V. Ippolito⁵⁷, A. Irles Quiles¹⁶⁸, C. Isaksson¹⁶⁷, M. Ishino⁶⁷, M. Ishitsuka¹⁵⁸, R. Ishmukhametov¹¹⁰, C. Issever¹¹⁹, S. Istin^{19a}, J.M. Iturbe Ponce⁸³, R. Iuppa^{134a,134b}, J. Ivarsson⁸⁰, W. Iwanski³⁹, H. Iwasaki⁶⁵, J.M. Izen⁴¹, V. Izzo^{103a}, B. Jackson¹²¹, M. Jackson⁷³, P. Jackson¹, M.R. Jaekel³⁰, V. Jain², K. Jakobs⁴⁸, S. Jakobsen³⁰, T. Jakoubek¹²⁶, J. Jakubek¹²⁷, D.O. Jamin¹⁵², D.K. Jana⁷⁸, E. Jansen⁷⁷, H. Jansen³⁰, J. Janssen²¹, M. Janus¹⁷¹, G. Jarlskog⁸⁰, N. Javadov^{64,b}, T. Javůrek⁴⁸, L. Jeanty¹⁵, J. Jejelava^{51a,r}, G.-Y. Jeng¹⁵¹, D. Jennens⁸⁷, P. Jenni^{48,s}, J. Jentzsch⁴³, C. Jeske¹⁷¹, S. Jézéquel⁵, H. Ji¹⁷⁴, J. Jia¹⁴⁹, Y. Jiang^{33b}, M. Jimenez Belenguer⁴², S. Jin^{33a}, A. Jinaru^{26a}, O. Jinnouchi¹⁵⁸, M.D. Joergensen³⁶, K.E. Johansson^{147a,147b}, P. Johansson¹⁴⁰, K.A. Johns⁷, K. Jon-And^{147a,147b}, G. Jones¹⁷¹, R.W.L. Jones⁷¹, T.J. Jones⁷³, J. Jongmanns^{58a}, P.M. Jorge^{125a,125b}, K.D. Joshi⁸³, J. Jovicevic¹⁴⁸, X. Ju¹⁷⁴, C.A. Jung⁴³, R.M. Jungst³⁰, P. Jussel⁶¹, A. Juste Rozas^{12,p}, M. Kaci¹⁶⁸, A. Kaczmarska³⁹, M. Kado¹¹⁶, H. Kagan¹¹⁰, M. Kagan¹⁴⁴, E. Kajomovitz⁴⁵, C.W. Kalderon¹¹⁹, S. Kama⁴⁰, A. Kamenshchikov¹²⁹, N. Kanaya¹⁵⁶, M. Kaneda³⁰, S. Kaneti²⁸, V.A. Kantserov⁹⁷, J. Kanzaki⁶⁵, B. Kaplan¹⁰⁹, A. Kapliy³¹, D. Kar⁵³, K. Karakostas¹⁰, N. Karastathis¹⁰, M. Karnevskiy⁸², S.N. Karpov⁶⁴, Z.M. Karpova⁶⁴, K. Karthik¹⁰⁹, V. Kartvelishvili⁷¹, A.N. Karyukhin¹²⁹, L. Kashif¹⁷⁴, G. Kasieczka^{58b}, R.D. Kass¹¹⁰, A. Kastanas¹⁴, Y. Kataoka¹⁵⁶, A. Katre⁴⁹, J. Katzy⁴², V. Kaushik⁷, K. Kawagoe⁶⁹, T. Kawamoto¹⁵⁶, G. Kawamura⁵⁴, S. Kazama¹⁵⁶, V.F. Kazanin^{108,c}, M.Y. Kazarinov⁶⁴, R. Keeler¹⁷⁰, R. Kehoe⁴⁰, J.S. Keller⁴², J.J. Kempster⁷⁶, H. Keoshkerian⁵, O. Kepka¹²⁶, B.P. Kerševan⁷⁴, S. Kersten¹⁷⁶, K. Kessoku¹⁵⁶, J. Keung¹⁵⁹, F. Khalil-zada¹¹, H. Khandanyan^{147a,147b}, A. Khanov¹¹³, A. Khodinov⁹⁷, A. Khomich^{58a}, T.J. Khoo²⁸, G. Khoriauli²¹, A. Khoroshilov¹⁷⁶, V. Khovanskiy⁹⁶, E. Khramov⁶⁴, J. Khubua^{51b,t}, H.Y. Kim⁸, H. Kim^{147a,147b}, S.H. Kim¹⁶¹, N. Kimura¹⁷², O.M. Kind¹⁶, B.T. King⁷³, M. King¹⁶⁸, R.S.B. King¹¹⁹, S.B. King¹⁶⁹, J. Kirk¹³⁰, A.E. Kiryunin¹⁰⁰, T. Kishimoto⁶⁶, D. Kisielewska^{38a}, F. Kiss⁴⁸, T. Kittelmann¹²⁴, K. Kiuchi¹⁶¹, E. Kladiva^{145b}, M. Klein⁷³, U. Klein⁷³, K. Kleinknecht⁸²,

P. Klimek^{147a,147b}, A. Klimentov²⁵, R. Klingenberg⁴³, J.A. Klinger⁸³, T. Klioutchnikova³⁰, P.F. Klok¹⁰⁵, E.-E. Kluge^{58a}, P. Kluit¹⁰⁶, S. Kluth¹⁰⁰, E. Knerner⁶¹, E.B.F.G. Knoops⁸⁴, A. Knue⁵³, D. Kobayashi¹⁵⁸, T. Kobayashi¹⁵⁶, M. Kobel⁴⁴, M. Kocian¹⁴⁴, P. Kodys¹²⁸, P. Koevesarki²¹, T. Koffas²⁹, E. Koffeman¹⁰⁶, L.A. Kogan¹¹⁹, S. Kohlmann¹⁷⁶, Z. Kohout¹²⁷, T. Kohriki⁶⁵, T. Koi¹⁴⁴, H. Kolanoski¹⁶, I. Koletsou⁵, J. Koll⁸⁹, A.A. Komar^{95,*}, Y. Komori¹⁵⁶, T. Kondo⁶⁵, N. Kondrashova⁴², K. Köneke⁴⁸, A.C. König¹⁰⁵, S. König⁸², T. Kono^{65,u}, R. Konoplich^{109,v}, N. Konstantinidis⁷⁷, R. Kopeliansky¹⁵³, S. Koperny^{38a}, L. Köpke⁸², A.K. Kopp⁴⁸, K. Korcyl³⁹, K. Kordas¹⁵⁵, A. Korn⁷⁷, A.A. Korol^{108,c}, I. Korolkov¹², E.V. Korolkova¹⁴⁰, V.A. Korotkov¹²⁹, O. Kortner¹⁰⁰, S. Kortner¹⁰⁰, V.V. Kostyukhin²¹, V.M. Kotov⁶⁴, A. Kotwal⁴⁵, C. Kourkoumelis⁹, V. Kouskoura¹⁵⁵, A. Koutsman^{160a}, R. Kowalewski¹⁷⁰, T.Z. Kowalski^{38a}, W. Kozanecki¹³⁷, A.S. Kozhin¹²⁹, V. Kral¹²⁷, V.A. Kramarenko⁹⁸, G. Kramberger⁷⁴, D. Krasnopenvtsev⁹⁷, M.W. Krasny⁷⁹, A. Krasznahorkay³⁰, J.K. Kraus²¹, A. Kravchenko²⁵, S. Kreiss¹⁰⁹, M. Kretz^{58c}, J. Kretzschmar⁷³, K. Kreutzfeldt⁵², P. Krieger¹⁵⁹, K. Kroeninger⁵⁴, H. Kroha¹⁰⁰, J. Kroll¹²¹, J. Kroseberg²¹, J. Krstic^{13a}, U. Kruchonak⁶⁴, H. Krüger²¹, T. Kruker¹⁷, N. Krumnack⁶³, Z.V. Krumshteyn⁶⁴, A. Kruse¹⁷⁴, M.C. Kruse⁴⁵, M. Kruskal²², T. Kubota⁸⁷, S. Kuday^{4a}, S. Kuehn⁴⁸, A. Kugel^{58c}, A. Kuhl¹³⁸, T. Kuhl⁴², V. Kukhtin⁶⁴, Y. Kulchitsky⁹¹, S. Kuleshov^{32b}, M. Kuna^{133a,133b}, J. Kunkle¹²¹, A. Kupco¹²⁶, H. Kurashige⁶⁶, Y.A. Kurochkin⁹¹, R. Kurumida⁶⁶, V. Kus¹²⁶, E.S. Kuwertz¹⁴⁸, M. Kuze¹⁵⁸, J. Kvita¹¹⁴, A. La Rosa⁴⁹, L. La Rotonda^{37a,37b}, C. Lacasta¹⁶⁸, F. Lacava^{133a,133b}, J. Lacey²⁹, H. Lacker¹⁶, D. Lacour⁷⁹, V.R. Lacuesta¹⁶⁸, E. Ladygin⁶⁴, R. Lafaye⁵, B. Laforge⁷⁹, T. Lagouri¹⁷⁷, S. Lai⁴⁸, H. Laier^{58a}, L. Lambourne⁷⁷, S. Lammers⁶⁰, C.L. Lampen⁷, W. Lampl⁷, E. Lançon¹³⁷, U. Landgraf⁴⁸, M.P.J. Landon⁷⁵, V.S. Lang^{58a}, A.J. Lankford¹⁶⁴, F. Lanni²⁵, K. Lantzsch³⁰, S. Laplace⁷⁹, C. Lapoire²¹, J.F. Laporte¹³⁷, T. Lari^{90a}, M. Lassnig³⁰, P. Laurelli⁴⁷, W. Lavrijsen¹⁵, A.T. Law¹³⁸, P. Laycock⁷³, O. Le Dortz⁷⁹, E. Le Guiriec⁸⁴, E. Le Menedeu¹², T. LeCompte⁶, F. Ledroit-Guillon⁵⁵, C.A. Lee¹⁵², H. Lee¹⁰⁶, J.S.H. Lee¹¹⁷, S.C. Lee¹⁵², L. Lee¹⁷⁷, G. Lefebvre⁷⁹, M. Lefebvre¹⁷⁰, F. Legger⁹⁹, C. Leggett¹⁵, A. Lehan⁷³, M. Lehmaccher²¹, G. Lehmann Miotto³⁰, X. Lei⁷, W.A. Leight²⁹, A. Leisos^{155,w}, A.G. Leister¹⁷⁷, M.A.L. Leite^{24d}, R. Leitner¹²⁸, D. Lellouch¹⁷³, B. Lemmer⁵⁴, K.J.C. Leney⁷⁷, T. Lenz²¹, B. Lenzi³⁰, R. Leone⁷, S. Leone^{123a,123b}, K. Leonhardt⁴⁴, C. Leonidopoulos⁴⁶, S. Leontsinis¹⁰, C. Leroy⁹⁴, C.G. Lester²⁸, C.M. Lester¹²¹, M. Levchenko¹²², J. Levêque⁵, D. Levin⁸⁸, L.J. Levinson¹⁷³, M. Levy¹⁸, A. Lewis¹¹⁹, G.H. Lewis¹⁰⁹, A.M. Leyko²¹, M. Leyton⁴¹, B. Li^{33b,x}, B. Li⁸⁴, H. Li¹⁴⁹, H.L. Li³¹, L. Li⁴⁵, L. Li^{33e}, S. Li⁴⁵, Y. Li^{33c,y}, Z. Liang¹³⁸, H. Liao³⁴, B. Liberti^{134a}, P. Lichard³⁰, K. Lie¹⁶⁶, J. Liebal²¹, W. Liebig¹⁴, C. Limbach²¹, A. Limosani⁸⁷, S.C. Lin^{152,z}, T.H. Lin⁸², F. Linde¹⁰⁶, B.E. Lindquist¹⁴⁹, J.T. Linnemann⁸⁹, E. Lipeles¹²¹, A. Lipniacka¹⁴, M. Lisovyi⁴², T.M. Liss¹⁶⁶, D. Lissauer²⁵, A. Lister¹⁶⁹, A.M. Litke¹³⁸, B. Liu^{152,aa}, D. Liu¹⁵², J.B. Liu^{33b}, K. Liu^{33b,ab}, L. Liu⁸⁸, M. Liu⁴⁵, M. Liu^{33b}, Y. Liu^{33b}, M. Livan^{120a,120b}, S.S.A. Livermore¹¹⁹, A. Lleres⁵⁵, J. Llorente Merino⁸¹, S.L. Lloyd⁷⁵, F. Lo Sterzo¹⁵², E. Lobodzinska⁴², P. Loch⁷, W.S. Lockman¹³⁸, F.K. Loebinger⁸³, A.E. Loevschall-Jensen³⁶, A. Loginov¹⁷⁷, T. Lohse¹⁶, K. Lohwasser⁴², M. Lokajicek¹²⁶, V.P. Lombardo⁵, B.A. Long²², J.D. Long⁸⁸, R.E. Long⁷¹, L. Lopes^{125a}, D. Lopez Mateos⁵⁷, B. Lopez Paredes¹⁴⁰, I. Lopez Paz¹², J. Lorenz⁹⁹, N. Lorenzo Martinez⁶⁰, M. Losada¹⁶³, P. Loscutoff¹⁵, X. Lou⁴¹, A. Lounis¹¹⁶, J. Love⁶, P.A. Love⁷¹, A.J. Lowe^{144,f}, N. Lu⁸⁸, H.J. Lubatti¹³⁹, C. Luci^{133a,133b}, A. Lucotte⁵⁵, F. Luehring⁶⁰, W. Lukas⁶¹, L. Luminari^{133a}, O. Lundberg^{147a,147b}, B. Lund-Jensen¹⁴⁸, M. Lungwitz⁸², D. Lynn²⁵, R. Lysak¹²⁶, E. Lytken⁸⁰, H. Ma²⁵, L.L. Ma^{33d}, G. Maccarrone⁴⁷, A. Macchiolo¹⁰⁰, J. Machado Miguens^{125a,125b}, D. Macina³⁰, D. Madaffari⁸⁴, R. Madar⁴⁸, H.J. Maddocks⁷¹, W.F. Mader⁴⁴, A. Madsen¹⁶⁷, T. Maeno²⁵, M. Maeno Kataoka⁸, E. Magradze⁵⁴, K. Mahboubi⁴⁸, J. Mahlstedt¹⁰⁶, S. Mahmoud⁷³, C. Maiani¹³⁷, C. Maidantchik^{24a}, A.A. Maier¹⁰⁰, A. Maio^{125a,125b,125d}, S. Majewski¹¹⁵, Y. Makida⁶⁵, N. Makovec¹¹⁶, P. Mal^{137,ac}, B. Malaescu⁷⁹, Pa. Malecki³⁹, V.P. Maleev¹²², F. Malek⁵⁵, U. Mallik⁶², D. Malon⁶, C. Malone¹⁴⁴, S. Maltezos¹⁰, V.M. Malyshev¹⁰⁸, S. Malyukov³⁰, J. Mamuzic¹³, B. Mandelli³⁰, L. Mandelli^{90a}, I. Mandic⁷⁴, R. Mandrysch⁶², J. Maneira^{125a,125b}, A. Manfredini¹⁰⁰, L. Manhaes de Andrade Filho^{24b}, J. Manjarres Ramos^{160b}, A. Mann⁹⁹, P.M. Manning¹³⁸, A. Manousakis-Katsikakis⁹, B. Mansoulie¹³⁷, R. Mantifel⁸⁶, L. Mapelli³⁰, L. March^{146c}, J.F. Marchand²⁹, G. Marchiori⁷⁹, M. Marcisovsky¹²⁶, C.P. Marino¹⁷⁰, M. Marjanovic^{13a}, C.N. Marques^{125a}, F. Marroquim^{24a}, S.P. Marsden⁸³, Z. Marshall¹⁵, L.F. Marti¹⁷, S. Marti-Garcia¹⁶⁸, B. Martin³⁰, B. Martin⁸⁹, T.A. Martin¹⁷¹, V.J. Martin⁴⁶, B. Martin dit Latour¹⁴, H. Martinez¹³⁷, M. Martinez^{12,p}, S. Martin-Haugh¹³⁰, A.C. Martyniuk⁷⁷,

M. Marx¹³⁹, F. Marzano^{133a}, A. Marzin³⁰, L. Masetti⁸², T. Mashimo¹⁵⁶, R. Mashinistov⁹⁵, J. Masik⁸³,
 A.L. Maslenikov^{108,c}, I. Massa^{20a,20b}, L. Massa^{20a,20b}, N. Massol⁵, P. Mastrandrea¹⁴⁹,
 A. Mastroberardino^{37a,37b}, T. Masubuchi¹⁵⁶, P. Mättig¹⁷⁶, J. Mattmann⁸², J. Maurer^{26a}, S.J. Maxfield⁷³,
 D.A. Maximov^{108,c}, R. Mazini¹⁵², L. Mazzaferro^{134a,134b}, G. Mc Goldrick¹⁵⁹, S.P. Mc Kee⁸⁸, A. McCarn⁸⁸,
 R.L. McCarthy¹⁴⁹, T.G. McCarthy²⁹, N.A. McCubbin¹³⁰, K.W. McFarlane^{56,*}, J.A. Mcfayden⁷⁷,
 G. Mchedlidze⁵⁴, S.J. McMahon¹³⁰, R.A. McPherson^{170,l}, A. Meade⁸⁵, J. Mechnick¹⁰⁶, M. Medinnis⁴²,
 S. Meehan³¹, S. Mehlhase⁹⁹, A. Mehta⁷³, K. Meier^{58a}, C. Meineck⁹⁹, B. Meirose⁸⁰, C. Melachrinos³¹,
 B.R. Mellado Garcia^{146c}, F. Meloni¹⁷, A. Mengarelli^{20a,20b}, S. Menke¹⁰⁰, E. Meoni¹⁶², K.M. Mercurio⁵⁷,
 S. Mergelmeyer²¹, N. Meric¹³⁷, P. Mermod⁴⁹, L. Merola^{103a,103b}, C. Meroni^{90a}, F.S. Merritt³¹,
 H. Merritt¹¹⁰, A. Messina^{30,ad}, J. Metcalfe²⁵, A.S. Mete¹⁶⁴, C. Meyer⁸², C. Meyer¹²¹, J-P. Meyer¹³⁷,
 J. Meyer³⁰, R.P. Middleton¹³⁰, S. Migas⁷³, L. Mijović²¹, G. Mikenberg¹⁷³, M. Mikestikova¹²⁶, M. Mikuž⁷⁴,
 A. Milic³⁰, D.W. Miller³¹, C. Mills⁴⁶, A. Milov¹⁷³, D.A. Milstead^{147a,147b}, D. Milstein¹⁷³,
 A.A. Minaenko¹²⁹, I.A. Minashvili⁶⁴, A.I. Mincer¹⁰⁹, B. Mindur^{38a}, M. Mineev⁶⁴, Y. Ming¹⁷⁴, L.M. Mir¹²,
 G. Mirabelli^{133a}, T. Mitani¹⁷², J. Mitrevski⁹⁹, V.A. Mitsou¹⁶⁸, S. Mitsui⁶⁵, A. Miucci⁴⁹, P.S. Miyagawa¹⁴⁰,
 J.U. Mjörnmark⁸⁰, T. Moa^{147a,147b}, K. Mochizuki⁸⁴, S. Mohapatra³⁵, W. Mohr⁴⁸, S. Molander^{147a,147b},
 R. Moles-Valls¹⁶⁸, K. Mönig⁴², C. Monini⁵⁵, J. Monk³⁶, E. Monnier⁸⁴, J. Montejo Berlingen¹²,
 F. Monticelli⁷⁰, S. Monzani^{133a,133b}, R.W. Moore³, A. Moraes⁵³, N. Morange⁶², D. Moreno⁸²,
 M. Moreno Llácer⁵⁴, P. Morettini^{50a}, M. Morgenstern⁴⁴, M. Morii⁵⁷, S. Moritz⁸², A.K. Morley¹⁴⁸,
 G. Mornacchi³⁰, J.D. Morris⁷⁵, L. Morvaj¹⁰², H.G. Moser¹⁰⁰, M. Mosidze^{51b}, J. Moss¹¹⁰, K. Motohashi¹⁵⁸,
 R. Mount¹⁴⁴, E. Mountricha²⁵, S.V. Mouraviev^{95,*}, E.J.W. Moyse⁸⁵, S. Muanza⁸⁴, R.D. Mudd¹⁸,
 F. Mueller^{58a}, J. Mueller¹²⁴, K. Mueller²¹, T. Mueller²⁸, T. Mueller⁸², D. Muenstermann⁴⁹, Y. Munwes¹⁵⁴,
 J.A. Murillo Quijada¹⁸, W.J. Murray^{171,130}, H. Musheghyan⁵⁴, E. Musto¹⁵³, A.G. Myagkov^{129,ae},
 M. Myska¹²⁷, O. Nackenhorst⁵⁴, J. Nadal⁵⁴, K. Nagai⁶¹, R. Nagai¹⁵⁸, Y. Nagai⁸⁴, K. Nagano⁶⁵,
 A. Nagarkar¹¹⁰, Y. Nagasaka⁵⁹, M. Nagel¹⁰⁰, A.M. Nairz³⁰, Y. Nakahama³⁰, K. Nakamura⁶⁵,
 T. Nakamura¹⁵⁶, I. Nakano¹¹¹, H. Namasivayam⁴¹, G. Nanava²¹, R. Narayan^{58b}, T. Nattermann²¹,
 T. Naumann⁴², G. Navarro¹⁶³, R. Nayyar⁷, H.A. Neal⁸⁸, P.Yu. Nechaeva⁹⁵, T.J. Neep⁸³, P.D. Nef¹⁴⁴,
 A. Negri^{120a,120b}, G. Negri³⁰, M. Negrini^{20a}, S. Nektarijevic⁴⁹, A. Nelson¹⁶⁴, T.K. Nelson¹⁴⁴,
 S. Nemecek¹²⁶, P. Nemethy¹⁰⁹, A.A. Nepomuceno^{24a}, M. Nessi^{30,af}, M.S. Neubauer¹⁶⁶, M. Neumann¹⁷⁶,
 R.M. Neves¹⁰⁹, P. Nevski²⁵, P.R. Newman¹⁸, D.H. Nguyen⁶, R.B. Nickerson¹¹⁹, R. Nicolaïdou¹³⁷,
 B. Nicquevert³⁰, J. Nielsen¹³⁸, N. Nikiforou³⁵, A. Nikiforov¹⁶, V. Nikolaenko^{129,ae}, I. Nikolic-Audit⁷⁹,
 K. Nikolic⁴⁹, K. Nikolopoulos¹⁸, P. Nilsson⁸, Y. Ninomiya¹⁵⁶, A. Nisati^{133a}, R. Nisius¹⁰⁰, T. Nobe¹⁵⁸,
 L. Nodulman⁶, M. Nomachi¹¹⁷, I. Nomidis²⁹, S. Norberg¹¹², M. Nordberg³⁰, O. Novgorodova⁴⁴,
 S. Nowak¹⁰⁰, M. Nozaki⁶⁵, L. Nozka¹¹⁴, K. Ntekas¹⁰, G. Nunes Hanninger⁸⁷, T. Nunnemann⁹⁹, E. Nurse⁷⁷,
 F. Nuti⁸⁷, B.J. O'Brien⁴⁶, F. O'grady⁷, D.C. O'Neil¹⁴³, V. O'Shea⁵³, F.G. Oakham^{29,e}, H. Oberlack¹⁰⁰,
 T. Obermann²¹, J. Ocariz⁷⁹, A. Ochi⁶⁶, I. Ochoa⁷⁷, S. Oda⁶⁹, S. Odaka⁶⁵, H. Ogren⁶⁰, A. Oh⁸³, S.H. Oh⁴⁵,
 C.C. Ohm¹⁵, H. Ohman¹⁶⁷, W. Okamura¹¹⁷, H. Okawa²⁵, Y. Okumura³¹, T. Okuyama¹⁵⁶, A. Olariu^{26a},
 A.G. Olchevski⁶⁴, S.A. Olivares Pino⁴⁶, D. Oliveira Damazio²⁵, E. Oliver Garcia¹⁶⁸, A. Olszewski³⁹,
 J. Olszowska³⁹, A. Onofre^{125a,125e}, P.U.E. Onyisi^{31,q}, C.J. Oram^{160a}, M.J. Oreglia³¹, Y. Oren¹⁵⁴,
 D. Orestano^{135a,135b}, N. Orlando^{72a,72b}, C. Oropeza Barrera⁵³, R.S. Orr¹⁵⁹, B. Osculati^{50a,50b},
 R. Ospanov¹²¹, G. Otero y Garzon²⁷, H. Otono⁶⁹, M. Ouchrif^{136d}, E.A. Ouellette¹⁷⁰, F. Ould-Saada¹¹⁸,
 A. Ouraou¹³⁷, K.P. Oussoren¹⁰⁶, Q. Ouyang^{33a}, A. Ovcharova¹⁵, M. Owen⁸³, V.E. Ozcan^{19a}, N. Ozturk⁸,
 K. Pachal¹¹⁹, A. Pacheco Pages¹², C. Padilla Aranda¹², M. Pagáčová⁴⁸, S. Pagan Griso¹⁵, E. Paganis¹⁴⁰,
 C. Pahl¹⁰⁰, F. Paige²⁵, P. Pais⁸⁵, K. Pajchel¹¹⁸, G. Palacino^{160b}, S. Palestini³⁰, M. Palka^{38b}, D. Pallin³⁴,
 A. Palma^{125a,125b}, J.D. Palmer¹⁸, Y.B. Pan¹⁷⁴, E. Panagiotopoulou¹⁰, J.G. Panduro Vazquez⁷⁶, P. Pani¹⁰⁶,
 N. Panikashvili⁸⁸, S. Panitkin²⁵, D. Pantea^{26a}, L. Paolozzi^{134a,134b}, Th.D. Papadopoulou¹⁰,
 K. Papageorgiou¹⁵⁵, A. Paramonov⁶, D. Paredes Hernandez³⁴, M.A. Parker²⁸, F. Parodi^{50a,50b},
 J.A. Parsons³⁵, U. Parzefall⁴⁸, E. Pasqualucci^{133a}, S. Passaggio^{50a}, A. Passeri^{135a}, F. Pastore^{135a,135b,*},
 Fr. Pastore⁷⁶, G. Pásztor²⁹, S. Pataraia¹⁷⁶, N.D. Patel¹⁵¹, J.R. Pater⁸³, S. Patricelli^{103a,103b}, T. Pauly³⁰,
 J. Pearce¹⁷⁰, M. Pedersen¹¹⁸, S. Pedraza Lopez¹⁶⁸, R. Pedro^{125a,125b}, S.V. Peleganchuk^{108,c}, D. Pelikan¹⁶⁷,
 H. Peng^{33b}, B. Penning³¹, J. Penwell⁶⁰, D.V. Perepelitsa²⁵, E. Perez Codina^{160a},
 M.T. Pérez García-Estañ¹⁶⁸, V. Perez Reale³⁵, L. Perini^{90a,90b}, H. Pernegger³⁰, R. Perrino^{72a},
 R. Peschke⁴², V.D. Peshekhanov⁶⁴, K. Peters³⁰, R.F.Y. Peters⁸³, B.A. Petersen³⁰, T.C. Petersen³⁶,

E. Petit⁴², A. Petridis^{147a,147b}, C. Petridou¹⁵⁵, E. Petrolo^{133a}, F. Petrucci^{135a,135b}, N.E. Pettersson¹⁵⁸, R. Pezoa^{32b}, P.W. Phillips¹³⁰, G. Piacquadio¹⁴⁴, E. Pianori¹⁷¹, A. Picazio⁴⁹, E. Piccaro⁷⁵, M. Piccinini^{20a,20b}, R. Piegai²⁷, D.T. Pignotti¹¹⁰, J.E. Pilcher³¹, A.D. Pilkington⁷⁷, J. Pina^{125a,125b,125d}, M. Pinamonti^{165a,165c,ag}, A. Pinder¹¹⁹, J.L. Pinfold³, A. Pingel³⁶, B. Pinto^{125a}, S. Pires⁷⁹, M. Pitt¹⁷³, C. Pizio^{90a,90b}, L. Plazak^{145a}, M.-A. Pleier²⁵, V. Pleskot¹²⁸, E. Plotnikova⁶⁴, P. Plucinski^{147a,147b}, S. Poddar^{58a}, F. Podlyski³⁴, R. Poettgen⁸², L. Poggioli¹¹⁶, D. Pohl²¹, M. Pohl⁴⁹, G. Polesello^{120a}, A. Pollicchio^{37a,37b}, R. Polifka¹⁵⁹, A. Polimi^{20a}, C.S. Pollard⁴⁵, V. Polychronakos²⁵, K. Pommès³⁰, L. Pontecorvo^{133a}, B.G. Pope⁸⁹, G.A. Popeneciu^{26b}, D.S. Popovic^{13a}, A. Poppleton³⁰, X. Portell Bueso¹², S. Pospisil¹²⁷, K. Potamianos¹⁵, I.N. Potrap⁶⁴, C.J. Potter¹⁵⁰, C.T. Potter¹¹⁵, G. Poulard³⁰, J. Poveda⁶⁰, V. Pozdnyakov⁶⁴, P. Pralavorio⁸⁴, A. Pranko¹⁵, S. Prasad³⁰, R. Pravahan⁸, S. Prell⁶³, D. Price⁸³, J. Price⁷³, L.E. Price⁶, D. Prieur¹²⁴, M. Primavera^{72a}, M. Proissl⁴⁶, K. Prokofiev⁴⁷, F. Prokoshin^{32b}, E. Protopapadaki¹³⁷, S. Protopopescu²⁵, J. Proudfoot⁶, M. Przybycien^{38a}, H. Przysiezniak⁵, E. Ptacek¹¹⁵, D. Puddu^{135a,135b}, E. Pueschel⁸⁵, D. Puldon¹⁴⁹, M. Purohit^{25,ah}, P. Puzo¹¹⁶, J. Qian⁸⁸, G. Qin⁵³, Y. Qin⁸³, A. Quadt⁵⁴, D.R. Quarrie¹⁵, W.B. Quayle^{165a,165b}, M. Queitsch-Maitland⁸³, D. Quilty⁵³, A. Qureshi^{160b}, V. Radeka²⁵, V. Radescu⁴², S.K. Radhakrishnan¹⁴⁹, P. Radloff¹¹⁵, P. Rados⁸⁷, F. Ragusa^{90a,90b}, G. Rahal¹⁷⁹, S. Rajagopalan²⁵, M. Rammensee³⁰, A.S. Randle-Conde⁴⁰, C. Rangel-Smith¹⁶⁷, K. Rao¹⁶⁴, F. Rauscher⁹⁹, T.C. Rave⁴⁸, T. Ravenscroft⁵³, M. Raymond³⁰, A.L. Read¹¹⁸, N.P. Readioff⁷³, D.M. Rebuzzi^{120a,120b}, A. Redelbach¹⁷⁵, G. Redlinger²⁵, R. Reece¹³⁸, K. Reeves⁴¹, L. Rehnisch¹⁶, H. Reisin²⁷, M. Relich¹⁶⁴, C. Rembser³⁰, H. Ren^{33a}, Z.L. Ren¹⁵², A. Renaud¹¹⁶, M. Rescigno^{133a}, S. Resconi^{90a}, O.L. Rezanova^{108,c}, P. Reznicek¹²⁸, R. Rezvani⁹⁴, R. Richter¹⁰⁰, M. Ridel⁷⁹, P. Rieck¹⁶, J. Rieger⁵⁴, M. Rijssenbeek¹⁴⁹, A. Rimoldi^{120a,120b}, L. Rinaldi^{20a}, E. Ritsch⁶¹, I. Riu¹², F. Rizatdinova¹¹³, E. Rizvi⁷⁵, S.H. Robertson^{86,l}, A. Robichaud-Veronneau⁸⁶, D. Robinson²⁸, J.E.M. Robinson⁸³, A. Robson⁵³, C. Roda^{123a,123b}, L. Rodrigues³⁰, S. Roe³⁰, O. Røhne¹¹⁸, S. Rolli¹⁶², A. Romaniouk⁹⁷, M. Romano^{20a,20b}, E. Romero Adam¹⁶⁸, N. Rompotis¹³⁹, M. Ronzani⁴⁸, L. Roos⁷⁹, E. Ros¹⁶⁸, S. Rosati^{133a}, K. Rosbach⁴⁹, M. Rose⁷⁶, P. Rose¹³⁸, P.L. Rosendahl¹⁴, O. Rosenthal¹⁴², V. Rossetti^{147a,147b}, E. Rossi^{103a,103b}, L.P. Rossi^{50a}, R. Rosten¹³⁹, M. Rotaru^{26a}, I. Roth¹⁷³, J. Rothberg¹³⁹, D. Rousseau¹¹⁶, C.R. Royon¹³⁷, A. Rozanova⁸⁴, Y. Rozen¹⁵³, X. Ruan^{146c}, F. Rubbo¹², I. Rubinsky⁴², V.I. Rud⁹⁸, C. Rudolph⁴⁴, M.S. Rudolph¹⁵⁹, F. Rühr⁴⁸, A. Ruiz-Martinez³⁰, Z. Rurikova⁴⁸, N.A. Rusakovich⁶⁴, A. Ruschke⁹⁹, J.P. Rutherford⁷, N. Ruthmann⁴⁸, Y.F. Ryabov¹²², M. Rybar¹²⁸, G. Rybkin¹¹⁶, N.C. Ryder¹¹⁹, A.F. Saavedra¹⁵¹, S. Sacerdoti²⁷, A. Saddique³, I. Sadeh¹⁵⁴, H.F-W. Sadrozinski¹³⁸, R. Sadykov⁶⁴, F. Safai Tehrani^{133a}, H. Sakamoto¹⁵⁶, Y. Sakurai¹⁷², G. Salamanna^{135a,135b}, A. Salamon^{134a}, M. Saleem¹¹², D. Salek¹⁰⁶, P.H. Sales De Bruin¹³⁹, D. Salihagic¹⁰⁰, A. Salnikov¹⁴⁴, J. Salt¹⁶⁸, D. Salvatore^{37a,37b}, F. Salvatore¹⁵⁰, A. Salvucci¹⁰⁵, A. Salzburger³⁰, D. Sampsonidis¹⁵⁵, A. Sanchez^{103a,103b}, J. Sánchez¹⁶⁸, V. Sanchez Martinez¹⁶⁸, H. Sandaker¹⁴, R.L. Sandbach⁷⁵, H.G. Sander⁸², M.P. Sanders⁹⁹, M. Sandhoff¹⁷⁶, T. Sandoval²⁸, C. Sandoval¹⁶³, R. Sandstroem¹⁰⁰, D.P.C. Sankey¹³⁰, A. Sansoni⁴⁷, C. Santoni³⁴, R. Santonico^{134a,134b}, H. Santos^{125a}, I. Santoyo Castillo¹⁵⁰, K. Sapp¹²⁴, A. Sapronov⁶⁴, J.G. Saraiva^{125a,125d}, B. Sarrazin²¹, G. Sartisohn¹⁷⁶, O. Sasaki⁶⁵, Y. Sasaki¹⁵⁶, G. Sauvage^{5,*}, E. Sauvan⁵, P. Savard^{159,e}, D.O. Savu³⁰, C. Sawyer¹¹⁹, L. Sawyer^{78,o}, D.H. Saxon⁵³, J. Saxon¹²¹, C. Sbarra^{20a}, A. Sbrizzi³, T. Scanlon⁷⁷, D.A. Scannicchio¹⁶⁴, M. Scarcella¹⁵¹, V. Scarfone^{37a,37b}, J. Schaarschmidt¹⁷³, P. Schacht¹⁰⁰, D. Schaefer³⁰, R. Schaefer⁴², S. Schaepe²¹, S. Schaetzl^{58b}, U. Schäfer⁸², A.C. Schaffer¹¹⁶, D. Schaille⁹⁹, R.D. Schamberger¹⁴⁹, V. Scharf^{58a}, V.A. Schegelsky¹²², D. Scheirich¹²⁸, M. Schernau¹⁶⁴, M.I. Scherzer³⁵, C. Schiavi^{50a,50b}, J. Schieck⁹⁹, C. Schillo⁴⁸, M. Schioppa^{37a,37b}, S. Schlenker³⁰, E. Schmidt⁴⁸, K. Schmieden³⁰, C. Schmitt⁸², S. Schmitt^{58b}, B. Schneider¹⁷, Y.J. Schnellbach⁷³, U. Schnoor⁴⁴, L. Schoeffel¹³⁷, A. Schoening^{58b}, B.D. Schoenrock⁸⁹, A.L.S. Schorlemmer⁵⁴, M. Schott⁸², D. Schouten^{160a}, J. Schovancova²⁵, S. Schramm¹⁵⁹, M. Schreyer¹⁷⁵, C. Schroeder⁸², N. Schuh⁸², M.J. Schultens²¹, H.-C. Schultz-Coulon^{58a}, H. Schulz¹⁶, M. Schumacher⁴⁸, B.A. Schumm¹³⁸, Ph. Schune¹³⁷, C. Schwanenberger⁸³, A. Schwartzman¹⁴⁴, Ph. Schwegler¹⁰⁰, Ph. Schwemling¹³⁷, R. Schwienhorst⁸⁹, J. Schwindling¹³⁷, T. Schwindt²¹, M. Schwoerer⁵, F.G. Sciacca¹⁷, E. Scifo¹¹⁶, G. Sciolla²³, W.G. Scott¹³⁰, F. Scuri^{123a,123b}, F. Scutti²¹, J. Searcy⁸⁸, G. Sedov⁴², E. Sedykh¹²², S.C. Seidel¹⁰⁴, A. Seiden¹³⁸, F. Seifert¹²⁷, J.M. Seixas^{24a}, G. Sekhniaidze^{103a}, S.J. Sekula⁴⁰, K.E. Selbach⁴⁶, D.M. Seliverstov^{122,*}, G. Sellers⁷³, N. Semprini-Cesari^{120a,20b}, C. Serfon³⁰, L. Serin¹¹⁶, L. Serkin⁵⁴, T. Serre⁸⁴, R. Seuster^{160a}, H. Severini¹¹², T. Sfiligoj⁷⁴, F. Sforza¹⁰⁰, A. Sfyrla³⁰,

E. Shabalina⁵⁴, M. Shamim¹¹⁵, L.Y. Shan^{33a}, R. Shang¹⁶⁶, J.T. Shank²², M. Shapiro¹⁵, P.B. Shatalov⁹⁶, K. Shaw^{165a,165b}, C.Y. Shehu¹⁵⁰, P. Sherwood⁷⁷, L. Shi^{152,ai}, S. Shimizu⁶⁶, C.O. Shimmin¹⁶⁴, M. Shimojima¹⁰¹, M. Shiyakova⁶⁴, A. Shmeleva⁹⁵, M.J. Shochet³¹, D. Short¹¹⁹, S. Shrestha⁶³, E. Shulga⁹⁷, M.A. Shupe⁷, S. Shushkevich⁴², P. Sicho¹²⁶, O. Sidiropoulou¹⁵⁵, D. Sidorov¹¹³, A. Sidoti^{133a}, F. Siegert⁴⁴, Dj. Sijacki^{13a}, J. Silva^{125a,125d}, Y. Silver¹⁵⁴, D. Silverstein¹⁴⁴, S.B. Silverstein^{147a}, V. Simak¹²⁷, O. Simard⁵, Lj. Simic^{13a}, S. Simion¹¹⁶, E. Simioni⁸², B. Simmons⁷⁷, R. Simoniello^{90a,90b}, M. Simonyan³⁶, P. Sinervo¹⁵⁹, N.B. Sinev¹¹⁵, V. Sipica¹⁴², G. Siragusa¹⁷⁵, A. Sircar⁷⁸, A.N. Sisakyan^{64,*}, S.Yu. Sivoklokov⁹⁸, J. Sjölin^{147a,147b}, T.B. Sjursen¹⁴, H.P. Skottowe⁵⁷, K.Yu. Skovpen¹⁰⁸, P. Skubic¹¹², M. Slater¹⁸, T. Slavicek¹²⁷, K. Sliwa¹⁶², V. Smakhtin¹⁷³, B.H. Smart⁴⁶, L. Smestad¹⁴, S.Yu. Smirnov⁹⁷, Y. Smirnov⁹⁷, L.N. Smirnova^{98,aj}, O. Smirnova⁸⁰, K.M. Smith⁵³, M. Smizanska⁷¹, K. Smolek¹²⁷, A.A. Snesarev⁹⁵, G. Snidero⁷⁵, S. Snyder²⁵, R. Sobie^{170,l}, F. Socher⁴⁴, A. Soffer¹⁵⁴, D.A. Soh^{152,ai}, C.A. Solans³⁰, M. Solar¹²⁷, J. Solc¹²⁷, E.Yu. Soldatov⁹⁷, U. Soldevila¹⁶⁸, A.A. Solodkov¹²⁹, A. Soloshenko⁶⁴, O.V. Solovyanov¹²⁹, V. Solovyev¹²², P. Sommer⁴⁸, H.Y. Song^{33b}, N. Soni¹, A. Sood¹⁵, A. Sopczak¹²⁷, B. Sopko¹²⁷, V. Sopko¹²⁷, V. Sorin¹², M. Sosebee⁸, R. Soualah^{165a,165c}, P. Soueid⁹⁴, A.M. Soukharev^{108,c}, D. South⁴², S. Spagnolo^{72a,72b}, F. Spanò⁷⁶, W.R. Spearman⁵⁷, F. Spettel¹⁰⁰, R. Spighi^{20a}, G. Spigo³⁰, L.A. Spiller⁸⁷, M. Spousta¹²⁸, T. Spreitzer¹⁵⁹, B. Spurlock⁸, R.D. St. Denis^{53,*}, S. Staerz⁴⁴, J. Stahlman¹²¹, R. Stamen^{58a}, S. Stamm¹⁶, E. Stanecka³⁹, R.W. Stanek⁶, C. Stanescu^{135a}, M. Stanescu-Bellu⁴², M.M. Stanitzki⁴², S. Stapnes¹¹⁸, E.A. Starchenko¹²⁹, J. Stark⁵⁵, P. Staroba¹²⁶, P. Starovoitov⁴², R. Staszewski³⁹, P. Stavina^{145a,*}, P. Steinberg²⁵, B. Stelzer¹⁴³, H.J. Stelzer³⁰, O. Stelzer-Chilton^{160a}, H. Stenzel⁵², S. Stern¹⁰⁰, G.A. Stewart⁵³, J.A. Stillings²¹, M.C. Stockton⁸⁶, M. Stoebe⁸⁶, G. Stoica^{26a}, P. Stolte⁵⁴, S. Stonjek¹⁰⁰, A.R. Stradling⁸, A. Straessner⁴⁴, M.E. Stramaglia¹⁷, J. Strandberg¹⁴⁸, S. Strandberg^{147a,147b}, A. Strandlie¹¹⁸, E. Strauss¹⁴⁴, M. Strauss¹¹², P. Strizenec^{145b}, R. Ströhmer¹⁷⁵, D.M. Strom¹¹⁵, R. Stroynowski⁴⁰, S.A. Stucci¹⁷, B. Stugu¹⁴, N.A. Styles⁴², D. Su¹⁴⁴, J. Su¹²⁴, R. Subramaniam⁷⁸, A. Succurro¹², Y. Sugaya¹¹⁷, C. Suhr¹⁰⁷, M. Suk¹²⁷, V.V. Sulin⁹⁵, S. Sultansoy^{4c}, T. Sumida⁶⁷, S. Sun⁵⁷, X. Sun^{33a}, J.E. Sundermann⁴⁸, K. Suruliz¹⁴⁰, G. Susinno^{37a,37b}, M.R. Sutton¹⁵⁰, Y. Suzuki⁶⁵, M. Svatos¹²⁶, S. Swedish¹⁶⁹, M. Swiatlowski¹⁴⁴, I. Sykora^{145a}, T. Sykora¹²⁸, D. Ta⁸⁹, C. Taccini^{135a,135b}, K. Tackmann⁴², J. Taenzer¹⁵⁹, A. Taffard¹⁶⁴, R. Tafirout^{160a}, N. Taiblum¹⁵⁴, H. Takai²⁵, R. Takashima⁶⁸, H. Takeda⁶⁶, T. Takeshita¹⁴¹, Y. Takubo⁶⁵, M. Talby⁸⁴, A.A. Talyshев^{108,c}, J.Y.C. Tam¹⁷⁵, K.G. Tan⁸⁷, J. Tanaka¹⁵⁶, R. Tanaka¹¹⁶, S. Tanaka¹³², S. Tanaka⁶⁵, A.J. Tanasijczuk¹⁴³, B.B. Tannenwald¹¹⁰, N. Tannoury²¹, S. Tapprogge⁸², S. Tarem¹⁵³, F. Tarrade²⁹, G.F. Tartarelli^{90a}, P. Tas¹²⁸, M. Tasevsky¹²⁶, T. Tashiro⁶⁷, E. Tassi^{37a,37b}, A. Tavares Delgado^{125a,125b}, Y. Tayalati^{136d}, F.E. Taylor⁹³, G.N. Taylor⁸⁷, W. Taylor^{160b}, F.A. Teischinger³⁰, M. Teixeira Dias Castanheira⁷⁵, P. Teixeira-Dias⁷⁶, K.K. Temming⁴⁸, H. Ten Kate³⁰, P.K. Teng¹⁵², J.J. Teoh¹¹⁷, S. Terada⁶⁵, K. Terashi¹⁵⁶, J. Terron⁸¹, S. Terzo¹⁰⁰, M. Testa⁴⁷, R.J. Teuscher^{159,l}, J. Therhaag²¹, T. Theveneaux-Pelzer³⁴, J.P. Thomas¹⁸, J. Thomas-Wilsker⁷⁶, E.N. Thompson³⁵, P.D. Thompson¹⁸, P.D. Thompson¹⁵⁹, R.J. Thompson⁸³, A.S. Thompson⁵³, L.A. Thomsen³⁶, E. Thomson¹²¹, M. Thomson²⁸, W.M. Thong⁸⁷, R.P. Thun^{88,*}, F. Tian³⁵, M.J. Tibbetts¹⁵, V.O. Tikhomirov^{95,ak}, Yu.A. Tikhonov^{108,c}, S. Timoshenko⁹⁷, E. Tiouchichine⁸⁴, P. Tipton¹⁷⁷, S. Tisserant⁸⁴, T. Todorov^{5,*}, S. Todorova-Nova¹²⁸, B. Toggerson⁷, J. Tojo⁶⁹, S. Tokár^{145a}, K. Tokushuku⁶⁵, K. Tollefson⁸⁹, L. Tomlinson⁸³, M. Tomoto¹⁰², L. Tompkins³¹, K. Toms¹⁰⁴, N.D. Topilin⁶⁴, E. Torrence¹¹⁵, H. Torres¹⁴³, E. Torró Pastor¹⁶⁸, J. Toth^{84,al}, F. Touchard⁸⁴, D.R. Tovey¹⁴⁰, H.L. Tran¹¹⁶, T. Trefzger¹⁷⁵, L. Tremblet³⁰, A. Tricoli³⁰, I.M. Trigger^{160a}, S. Trincaz-Duvoid⁷⁹, M.F. Tripiana¹², W. Trischuk¹⁵⁹, B. Trocmé⁵⁵, C. Troncon^{90a}, M. Trottier-McDonald¹⁴³, M. Trovatelli^{135a,135b}, P. True⁸⁹, M. Trzebinski³⁹, A. Trzupek³⁹, C. Tsarouchas³⁰, J.C-L. Tseng¹¹⁹, P.V. Tsiareshka⁹¹, D. Tsionou¹³⁷, G. Tsipolitis¹⁰, N. Tsirintanis⁹, S. Tsiskaridze¹², V. Tsiskaridze⁴⁸, E.G. Tskhadadze^{51a}, I.I. Tsukerman⁹⁶, V. Tsulaia¹⁵, S. Tsuno⁶⁵, D. Tsybychev¹⁴⁹, A. Tudorache^{26a}, V. Tudorache^{26a}, A.N. Tuna¹²¹, S.A. Tupputi^{20a,20b}, S. Turchikhin^{98,aj}, D. Turecek¹²⁷, R. Turra^{90a,90b}, P.M. Tuts³⁵, A. Tykhonov⁴⁹, M. Tylmad^{147a,147b}, M. Tyndel¹³⁰, K. Uchida²¹, I. Ueda¹⁵⁶, R. Ueno²⁹, M. Ughetto⁸⁴, M. Ugland¹⁴, M. Uhlenbrock²¹, F. Ukegawa¹⁶¹, G. Una³⁰, A. Undrus²⁵, G. Unel¹⁶⁴, F.C. Ungaro⁴⁸, Y. Unno⁶⁵, C. Unverdorben⁹⁹, D. Urbaniec³⁵, P. Urquijo⁸⁷, G. Usai⁸, A. Usanova⁶¹, L. Vacavant⁸⁴, V. Vacek¹²⁷, B. Vachon⁸⁶, N. Valencic¹⁰⁶, S. Valentinetti^{20a,20b}, A. Valero¹⁶⁸, L. Valery³⁴, S. Valkar¹²⁸, E. Valladolid Gallego¹⁶⁸, S. Vallecorsa⁴⁹, J.A. Valls Ferrer¹⁶⁸, W. Van Den Wollenberg¹⁰⁶, P.C. Van Der Deijl¹⁰⁶,

R. van der Geer¹⁰⁶, H. van der Graaf¹⁰⁶, R. Van Der Leeuw¹⁰⁶, D. van der Ster³⁰, N. van Eldik³⁰, P. van Gemmeren⁶, J. Van Nieuwkoop¹⁴³, I. van Vulpen¹⁰⁶, M.C. van Woerden³⁰, M. Vanadia^{133a,133b}, W. Vandelli³⁰, R. Vanguri¹²¹, A. Vaniachine⁶, F. Vannucci⁷⁹, G. Vardanyan¹⁷⁸, R. Vari^{133a}, E.W. Varnes⁷, T. Varol⁸⁵, D. Varouchas⁷⁹, A. Vartapetian⁸, K.E. Varvell¹⁵¹, F. Vazeille³⁴, T. Vazquez Schroeder⁵⁴, J. Veatch⁷, F. Veloso^{125a,125c}, T. Velz²¹, S. Veneziano^{133a}, A. Ventura^{72a,72b}, D. Ventura⁸⁵, M. Venturi¹⁷⁰, N. Venturi¹⁵⁹, A. Venturini²³, V. Vercesi^{120a}, M. Verducci^{133a,133b}, W. Verkerke¹⁰⁶, J.C. Vermeulen¹⁰⁶, A. Vest⁴⁴, M.C. Vetterli^{143,e}, O. Viazlo⁸⁰, I. Vichou¹⁶⁶, T. Vickey^{146c,am}, O.E. Vickey Boeriu^{146c}, G.H.A. Viehhauser¹¹⁹, S. Viel¹⁶⁹, R. Vigne³⁰, M. Villa^{20a,20b}, M. Villaplana Perez^{90a,90b}, E. Vilucchi⁴⁷, M.G. Vincter²⁹, V.B. Vinogradov⁶⁴, J. Virzi¹⁵, I. Vivarelli¹⁵⁰, F. Vives Vaque³, S. Vlachos¹⁰, D. Vladoiu⁹⁹, M. Vlasak¹²⁷, A. Vogel²¹, M. Vogel^{32a}, P. Vokac¹²⁷, G. Volpi^{123a,123b}, M. Volpi⁸⁷, H. von der Schmitt¹⁰⁰, H. von Radziewski⁴⁸, E. von Toerne²¹, V. Vorobel¹²⁸, K. Vorobev⁹⁷, M. Vos¹⁶⁸, R. Voss³⁰, J.H. Vossebeld⁷³, N. Vranjes¹³⁷, M. Vranjes Milosavljevic¹⁰⁶, V. Vrba¹²⁶, M. Vreeswijk¹⁰⁶, T. Vu Anh⁴⁸, R. Vuillermet³⁰, I. Vukotic³¹, Z. Vykydal¹²⁷, P. Wagner²¹, W. Wagner¹⁷⁶, H. Wahlberg⁷⁰, S. Wahrmund⁴⁴, J. Wakabayashi¹⁰², J. Walder⁷¹, R. Walker⁹⁹, W. Walkowiak¹⁴², R. Wall¹⁷⁷, P. Waller⁷³, B. Walsh¹⁷⁷, C. Wang^{152,an}, C. Wang⁴⁵, F. Wang¹⁷⁴, H. Wang¹⁵, H. Wang⁴⁰, J. Wang⁴², J. Wang^{33a}, K. Wang⁸⁶, R. Wang¹⁰⁴, S.M. Wang¹⁵², T. Wang²¹, X. Wang¹⁷⁷, C. Wanotayaroj¹¹⁵, A. Warburton⁸⁶, C.P. Ward²⁸, D.R. Wardrope⁷⁷, M. Warsinsky⁴⁸, A. Washbrook⁴⁶, C. Wasicki⁴², P.M. Watkins¹⁸, A.T. Watson¹⁸, I.J. Watson¹⁵¹, M.F. Watson¹⁸, G. Watts¹³⁹, S. Watts⁸³, B.M. Waugh⁷⁷, S. Webb⁸³, M.S. Weber¹⁷, S.W. Weber¹⁷⁵, J.S. Webster³¹, A.R. Weidberg¹¹⁹, P. Weigell¹⁰⁰, B. Weinert⁶⁰, J. Weingarten⁵⁴, C. Weiser⁴⁸, H. Weits¹⁰⁶, P.S. Wells³⁰, T. Wenaus²⁵, D. Wendland¹⁶, Z. Weng^{152,ai}, T. Wengler³⁰, S. Wenig³⁰, N. Wermes²¹, M. Werner⁴⁸, P. Werner³⁰, M. Wessels^{58a}, J. Wetter¹⁶², K. Whalen²⁹, A. White⁸, M.J. White¹, R. White^{32b}, S. White^{123a,123b}, D. Whiteson¹⁶⁴, D. Wicke¹⁷⁶, F.J. Wickens¹³⁰, W. Wiedenmann¹⁷⁴, M. Wielers¹³⁰, P. Wienemann²¹, C. Wiglesworth³⁶, L.A.M. Wiik-Fuchs²¹, P.A. Wijeratne⁷⁷, A. Wildauer¹⁰⁰, M.A. Wildt^{42,ao}, H.G. Wilkens³⁰, J.Z. Will⁹⁹, H.H. Williams¹²¹, S. Williams²⁸, C. Willis⁸⁹, S. Willocq⁸⁵, A. Wilson⁸⁸, J.A. Wilson¹⁸, I. Wingerter-Seez⁵, F. Winkelmeier¹¹⁵, B.T. Winter²¹, M. Wittgen¹⁴⁴, T. Wittig⁴³, J. Wittkowski⁹⁹, S.J. Wollstadt⁸², M.W. Wolter³⁹, H. Wolters^{125a,125c}, B.K. Wosiek³⁹, J. Wotschack³⁰, M.J. Woudstra⁸³, K.W. Wozniak³⁹, M. Wright⁵³, M. Wu⁵⁵, S.L. Wu¹⁷⁴, X. Wu⁴⁹, Y. Wu⁸⁸, E. Wulf³⁵, T.R. Wyatt⁸³, B.M. Wynne⁴⁶, S. Xella³⁶, M. Xiao¹³⁷, D. Xu^{33a}, L. Xu^{33b,ap}, B. Yabsley¹⁵¹, S. Yacoob^{146b,aq}, R. Yakabe⁶⁶, M. Yamada⁶⁵, H. Yamaguchi¹⁵⁶, Y. Yamaguchi¹¹⁷, A. Yamamoto⁶⁵, K. Yamamoto⁶³, S. Yamamoto¹⁵⁶, T. Yamamura¹⁵⁶, T. Yamanaka¹⁵⁶, K. Yamauchi¹⁰², Y. Yamazaki⁶⁶, Z. Yan²², H. Yang^{33e}, H. Yang¹⁷⁴, U.K. Yang⁸³, Y. Yang¹¹⁰, S. Yanush⁹², L. Yao^{33a}, W-M. Yao¹⁵, Y. Yasu⁶⁵, E. Yatsenko⁴², K.H. Yau Wong²¹, J. Ye⁴⁰, S. Ye²⁵, I. Yeletskikh⁶⁴, A.L. Yen⁵⁷, E. Yildirim⁴², M. Yilmaz^{4b}, R. Yoosoofmiya¹²⁴, K. Yorita¹⁷², R. Yoshida⁶, K. Yoshihara¹⁵⁶, C. Young¹⁴⁴, C.J.S. Young³⁰, S. Youssef²², D.R. Yu¹⁵, J. Yu⁸, J.M. Yu⁸⁸, J. Yu¹¹³, L. Yuan⁶⁶, A. Yurkewicz¹⁰⁷, I. Yusuff^{28,ar}, B. Zabinski³⁹, R. Zaidan⁶², A.M. Zaitsev^{129,ae}, A. Zaman¹⁴⁹, S. Zambito²³, L. Zanello^{133a,133b}, D. Zanzi¹⁰⁰, C. Zeitnitz¹⁷⁶, M. Zeman¹²⁷, A. Zemla^{38a}, K. Zengel²³, O. Zenin¹²⁹, T. Ženiš^{145a}, D. Zerwas¹¹⁶, G. Zevi della Porta⁵⁷, D. Zhang⁸⁸, F. Zhang¹⁷⁴, H. Zhang⁸⁹, J. Zhang⁶, L. Zhang¹⁵², X. Zhang^{33d}, Z. Zhang¹¹⁶, Z. Zhao^{33b}, A. Zhemchugov⁶⁴, J. Zhong¹¹⁹, B. Zhou⁸⁸, L. Zhou³⁵, N. Zhou¹⁶⁴, C.G. Zhu^{33d}, H. Zhu^{33a}, J. Zhu⁸⁸, Y. Zhu^{33b}, X. Zhuang^{33a}, K. Zhukov⁹⁵, A. Zibell¹⁷⁵, D. Ziemińska⁶⁰, N.I. Zimine⁶⁴, C. Zimmermann⁸², R. Zimmermann²¹, S. Zimmermann²¹, S. Zimmermann⁴⁸, Z. Zinonos⁵⁴, M. Ziolkowski¹⁴², G. Zobernig¹⁷⁴, A. Zoccoli^{20a,20b}, M. zur Nedden¹⁶, G. Zurzolo^{103a,103b}, V. Zutshi¹⁰⁷, L. Zwalski³⁰.

¹ Department of Physics, University of Adelaide, Adelaide, Australia

² Physics Department, SUNY Albany, Albany NY, United States of America

³ Department of Physics, University of Alberta, Edmonton AB, Canada

⁴ ^(a) Department of Physics, Ankara University, Ankara; ^(b) Department of Physics, Gazi University, Ankara;

^(c) Division of Physics, TOBB University of Economics and Technology, Ankara; ^(d) Turkish Atomic Energy Authority, Ankara, Turkey

⁵ LAPP, CNRS/IN2P3 and Université Savoie Mont Blanc, Annecy-le-Vieux, France

⁶ High Energy Physics Division, Argonne National Laboratory, Argonne IL, United States of America

⁷ Department of Physics, University of Arizona, Tucson AZ, United States of America

- ⁸ Department of Physics, The University of Texas at Arlington, Arlington TX, United States of America
⁹ Physics Department, University of Athens, Athens, Greece
¹⁰ Physics Department, National Technical University of Athens, Zografou, Greece
¹¹ Institute of Physics, Azerbaijan Academy of Sciences, Baku, Azerbaijan
¹² Institut de Física d'Altes Energies and Departament de Física de la Universitat Autònoma de Barcelona, Barcelona, Spain
¹³ (a) Institute of Physics, University of Belgrade, Belgrade, Serbia
¹⁴ Department for Physics and Technology, University of Bergen, Bergen, Norway
¹⁵ Physics Division, Lawrence Berkeley National Laboratory and University of California, Berkeley CA, United States of America
¹⁶ Department of Physics, Humboldt University, Berlin, Germany
¹⁷ Albert Einstein Center for Fundamental Physics and Laboratory for High Energy Physics, University of Bern, Bern, Switzerland
¹⁸ School of Physics and Astronomy, University of Birmingham, Birmingham, United Kingdom
¹⁹ (a) Department of Physics, Bogazici University, Istanbul; (b) Department of Physics, Dogus University, Istanbul; (c) Department of Physics Engineering, Gaziantep University, Gaziantep, Turkey
²⁰ (a) INFN Sezione di Bologna; (b) Dipartimento di Fisica e Astronomia, Università di Bologna, Bologna, Italy
²¹ Physikalisches Institut, University of Bonn, Bonn, Germany
²² Department of Physics, Boston University, Boston MA, United States of America
²³ Department of Physics, Brandeis University, Waltham MA, United States of America
²⁴ (a) Universidade Federal do Rio De Janeiro COPPE/EE/IF, Rio de Janeiro; (b) Electrical Circuits Department, Federal University of Juiz de Fora (UFJF), Juiz de Fora; (c) Federal University of Sao Joao del Rei (UFSJ), Sao Joao del Rei; (d) Instituto de Física, Universidade de São Paulo, São Paulo, Brazil
²⁵ Physics Department, Brookhaven National Laboratory, Upton NY, United States of America
²⁶ (a) National Institute of Physics and Nuclear Engineering, Bucharest; (b) National Institute for Research and Development of Isotopic and Molecular Technologies, Physics Department, Cluj Napoca; (c) University Politehnica Bucharest, Bucharest; (d) West University in Timisoara, Timisoara, Romania
²⁷ Departamento de Física, Universidad de Buenos Aires, Buenos Aires, Argentina
²⁸ Cavendish Laboratory, University of Cambridge, Cambridge, United Kingdom
²⁹ Department of Physics, Carleton University, Ottawa ON, Canada
³⁰ CERN, Geneva, Switzerland
³¹ Enrico Fermi Institute, University of Chicago, Chicago IL, United States of America
³² (a) Departamento de Física, Pontificia Universidad Católica de Chile, Santiago; (b) Departamento de Física, Universidad Técnica Federico Santa María, Valparaíso, Chile
³³ (a) Institute of High Energy Physics, Chinese Academy of Sciences, Beijing; (b) Department of Modern Physics, University of Science and Technology of China, Anhui; (c) Department of Physics, Nanjing University, Jiangsu; (d) School of Physics, Shandong University, Shandong; (e) Department of Physics and Astronomy, Shanghai Key Laboratory for Particle Physics and Cosmology, Shanghai Jiao Tong University, Shanghai, China
³⁴ Laboratoire de Physique Corpusculaire, Clermont Université and Université Blaise Pascal and CNRS/IN2P3, Clermont-Ferrand, France
³⁵ Nevis Laboratory, Columbia University, Irvington NY, United States of America
³⁶ Niels Bohr Institute, University of Copenhagen, Kobenhavn, Denmark
³⁷ (a) INFN Gruppo Collegato di Cosenza, Laboratori Nazionali di Frascati; (b) Dipartimento di Fisica, Università della Calabria, Rende, Italy
³⁸ (a) AGH University of Science and Technology, Faculty of Physics and Applied Computer Science, Krakow; (b) Marian Smoluchowski Institute of Physics, Jagiellonian University, Krakow, Poland
³⁹ Institute of Nuclear Physics Polish Academy of Sciences, Krakow, Poland
⁴⁰ Physics Department, Southern Methodist University, Dallas TX, United States of America
⁴¹ Physics Department, University of Texas at Dallas, Richardson TX, United States of America
⁴² DESY, Hamburg and Zeuthen, Germany

- ⁴³ Institut für Experimentelle Physik IV, Technische Universität Dortmund, Dortmund, Germany
⁴⁴ Institut für Kern- und Teilchenphysik, Technische Universität Dresden, Dresden, Germany
⁴⁵ Department of Physics, Duke University, Durham NC, United States of America
⁴⁶ SUPA - School of Physics and Astronomy, University of Edinburgh, Edinburgh, United Kingdom
⁴⁷ INFN Laboratori Nazionali di Frascati, Frascati, Italy
⁴⁸ Fakultät für Mathematik und Physik, Albert-Ludwigs-Universität, Freiburg, Germany
⁴⁹ Section de Physique, Université de Genève, Geneva, Switzerland
⁵⁰ (a) INFN Sezione di Genova; (b) Dipartimento di Fisica, Università di Genova, Genova, Italy
⁵¹ (a) E. Andronikashvili Institute of Physics, Iv. Javakhishvili Tbilisi State University, Tbilisi; (b) High Energy Physics Institute, Tbilisi State University, Tbilisi, Georgia
⁵² II Physikalisches Institut, Justus-Liebig-Universität Giessen, Giessen, Germany
⁵³ SUPA - School of Physics and Astronomy, University of Glasgow, Glasgow, United Kingdom
⁵⁴ II Physikalisches Institut, Georg-August-Universität, Göttingen, Germany
⁵⁵ Laboratoire de Physique Subatomique et de Cosmologie, Université Grenoble-Alpes, CNRS/IN2P3, Grenoble, France
⁵⁶ Department of Physics, Hampton University, Hampton VA, United States of America
⁵⁷ Laboratory for Particle Physics and Cosmology, Harvard University, Cambridge MA, United States of America
⁵⁸ (a) Kirchhoff-Institut für Physik, Ruprecht-Karls-Universität Heidelberg, Heidelberg; (b) Physikalisches Institut, Ruprecht-Karls-Universität Heidelberg, Heidelberg; (c) ZITI Institut für technische Informatik, Ruprecht-Karls-Universität Heidelberg, Mannheim, Germany
⁵⁹ Faculty of Applied Information Science, Hiroshima Institute of Technology, Hiroshima, Japan
⁶⁰ Department of Physics, Indiana University, Bloomington IN, United States of America
⁶¹ Institut für Astro- und Teilchenphysik, Leopold-Franzens-Universität, Innsbruck, Austria
⁶² University of Iowa, Iowa City IA, United States of America
⁶³ Department of Physics and Astronomy, Iowa State University, Ames IA, United States of America
⁶⁴ Joint Institute for Nuclear Research, JINR Dubna, Dubna, Russia
⁶⁵ KEK, High Energy Accelerator Research Organization, Tsukuba, Japan
⁶⁶ Graduate School of Science, Kobe University, Kobe, Japan
⁶⁷ Faculty of Science, Kyoto University, Kyoto, Japan
⁶⁸ Kyoto University of Education, Kyoto, Japan
⁶⁹ Department of Physics, Kyushu University, Fukuoka, Japan
⁷⁰ Instituto de Física La Plata, Universidad Nacional de La Plata and CONICET, La Plata, Argentina
⁷¹ Physics Department, Lancaster University, Lancaster, United Kingdom
⁷² (a) INFN Sezione di Lecce; (b) Dipartimento di Matematica e Fisica, Università del Salento, Lecce, Italy
⁷³ Oliver Lodge Laboratory, University of Liverpool, Liverpool, United Kingdom
⁷⁴ Department of Physics, Jožef Stefan Institute and University of Ljubljana, Ljubljana, Slovenia
⁷⁵ School of Physics and Astronomy, Queen Mary University of London, London, United Kingdom
⁷⁶ Department of Physics, Royal Holloway University of London, Surrey, United Kingdom
⁷⁷ Department of Physics and Astronomy, University College London, London, United Kingdom
⁷⁸ Louisiana Tech University, Ruston LA, United States of America
⁷⁹ Laboratoire de Physique Nucléaire et de Hautes Energies, UPMC and Université Paris-Diderot and CNRS/IN2P3, Paris, France
⁸⁰ Fysiska institutionen, Lunds universitet, Lund, Sweden
⁸¹ Departamento de Física Teórica C-15, Universidad Autónoma de Madrid, Madrid, Spain
⁸² Institut für Physik, Universität Mainz, Mainz, Germany
⁸³ School of Physics and Astronomy, University of Manchester, Manchester, United Kingdom
⁸⁴ CPPM, Aix-Marseille Université and CNRS/IN2P3, Marseille, France
⁸⁵ Department of Physics, University of Massachusetts, Amherst MA, United States of America
⁸⁶ Department of Physics, McGill University, Montreal QC, Canada
⁸⁷ School of Physics, University of Melbourne, Victoria, Australia
⁸⁸ Department of Physics, The University of Michigan, Ann Arbor MI, United States of America

- ⁸⁹ Department of Physics and Astronomy, Michigan State University, East Lansing MI, United States of America
- ⁹⁰ ^(a) INFN Sezione di Milano; ^(b) Dipartimento di Fisica, Università di Milano, Milano, Italy
- ⁹¹ B.I. Stepanov Institute of Physics, National Academy of Sciences of Belarus, Minsk, Republic of Belarus
- ⁹² National Scientific and Educational Centre for Particle and High Energy Physics, Minsk, Republic of Belarus
- ⁹³ Department of Physics, Massachusetts Institute of Technology, Cambridge MA, United States of America
- ⁹⁴ Group of Particle Physics, University of Montreal, Montreal QC, Canada
- ⁹⁵ P.N. Lebedev Institute of Physics, Academy of Sciences, Moscow, Russia
- ⁹⁶ Institute for Theoretical and Experimental Physics (ITEP), Moscow, Russia
- ⁹⁷ National Research Nuclear University MEPhI, Moscow, Russia
- ⁹⁸ D.V. Skobeltsyn Institute of Nuclear Physics, M.V. Lomonosov Moscow State University, Moscow, Russia
- ⁹⁹ Fakultät für Physik, Ludwig-Maximilians-Universität München, München, Germany
- ¹⁰⁰ Max-Planck-Institut für Physik (Werner-Heisenberg-Institut), München, Germany
- ¹⁰¹ Nagasaki Institute of Applied Science, Nagasaki, Japan
- ¹⁰² Graduate School of Science and Kobayashi-Maskawa Institute, Nagoya University, Nagoya, Japan
- ¹⁰³ ^(a) INFN Sezione di Napoli; ^(b) Dipartimento di Fisica, Università di Napoli, Napoli, Italy
- ¹⁰⁴ Department of Physics and Astronomy, University of New Mexico, Albuquerque NM, United States of America
- ¹⁰⁵ Institute for Mathematics, Astrophysics and Particle Physics, Radboud University Nijmegen/Nikhef, Nijmegen, Netherlands
- ¹⁰⁶ Nikhef National Institute for Subatomic Physics and University of Amsterdam, Amsterdam, Netherlands
- ¹⁰⁷ Department of Physics, Northern Illinois University, DeKalb IL, United States of America
- ¹⁰⁸ Budker Institute of Nuclear Physics, SB RAS, Novosibirsk, Russia
- ¹⁰⁹ Department of Physics, New York University, New York NY, United States of America
- ¹¹⁰ Ohio State University, Columbus OH, United States of America
- ¹¹¹ Faculty of Science, Okayama University, Okayama, Japan
- ¹¹² Homer L. Dodge Department of Physics and Astronomy, University of Oklahoma, Norman OK, United States of America
- ¹¹³ Department of Physics, Oklahoma State University, Stillwater OK, United States of America
- ¹¹⁴ Palacký University, RCPTM, Olomouc, Czech Republic
- ¹¹⁵ Center for High Energy Physics, University of Oregon, Eugene OR, United States of America
- ¹¹⁶ LAL, Université Paris-Sud and CNRS/IN2P3, Orsay, France
- ¹¹⁷ Graduate School of Science, Osaka University, Osaka, Japan
- ¹¹⁸ Department of Physics, University of Oslo, Oslo, Norway
- ¹¹⁹ Department of Physics, Oxford University, Oxford, United Kingdom
- ¹²⁰ ^(a) INFN Sezione di Pavia; ^(b) Dipartimento di Fisica, Università di Pavia, Pavia, Italy
- ¹²¹ Department of Physics, University of Pennsylvania, Philadelphia PA, United States of America
- ¹²² National Research Centre "Kurchatov Institute" B.P.Konstantinov Petersburg Nuclear Physics Institute, St. Petersburg, Russia
- ¹²³ ^(a) INFN Sezione di Pisa; ^(b) Dipartimento di Fisica E. Fermi, Università di Pisa, Pisa, Italy
- ¹²⁴ Department of Physics and Astronomy, University of Pittsburgh, Pittsburgh PA, United States of America
- ¹²⁵ ^(a) Laboratorio de Instrumentacao e Fisica Experimental de Particulas - LIP, Lisboa; ^(b) Faculdade de Ciências, Universidade de Lisboa, Lisboa; ^(c) Department of Physics, University of Coimbra, Coimbra; ^(d) Centro de Física Nuclear da Universidade de Lisboa, Lisboa; ^(e) Departamento de Fisica, Universidade do Minho, Braga; ^(f) Departamento de Fisica Teorica y del Cosmos and CAFPE, Universidad de Granada, Granada (Spain); ^(g) Dep Fisica and CEFITEC of Faculdade de Ciencias e Tecnologia, Universidade Nova de Lisboa, Caparica, Portugal

- ¹²⁶ Institute of Physics, Academy of Sciences of the Czech Republic, Praha, Czech Republic
¹²⁷ Czech Technical University in Prague, Praha, Czech Republic
¹²⁸ Faculty of Mathematics and Physics, Charles University in Prague, Praha, Czech Republic
¹²⁹ State Research Center Institute for High Energy Physics, Protvino, Russia
¹³⁰ Particle Physics Department, Rutherford Appleton Laboratory, Didcot, United Kingdom
¹³¹ Physics Department, University of Regina, Regina SK, Canada
¹³² Ritsumeikan University, Kusatsu, Shiga, Japan
¹³³ ^(a) INFN Sezione di Roma; ^(b) Dipartimento di Fisica, Sapienza Università di Roma, Roma, Italy
¹³⁴ ^(a) INFN Sezione di Roma Tor Vergata; ^(b) Dipartimento di Fisica, Università di Roma Tor Vergata, Roma, Italy
¹³⁵ ^(a) INFN Sezione di Roma Tre; ^(b) Dipartimento di Matematica e Fisica, Università Roma Tre, Roma, Italy
¹³⁶ ^(a) Faculté des Sciences Ain Chock, Réseau Universitaire de Physique des Hautes Energies - Université Hassan II, Casablanca; ^(b) Centre National de l'Energie des Sciences Techniques Nucleaires, Rabat; ^(c) Faculté des Sciences Semlalia, Université Cadi Ayyad, LPHEA-Marrakech; ^(d) Faculté des Sciences, Université Mohamed Premier and LPTPM, Oujda; ^(e) Faculté des sciences, Université Mohammed V-Agdal, Rabat, Morocco
¹³⁷ DSM/IRFU (Institut de Recherches sur les Lois Fondamentales de l'Univers), CEA Saclay (Commissariat à l'Energie Atomique et aux Energies Alternatives), Gif-sur-Yvette, France
¹³⁸ Santa Cruz Institute for Particle Physics, University of California Santa Cruz, Santa Cruz CA, United States of America
¹³⁹ Department of Physics, University of Washington, Seattle WA, United States of America
¹⁴⁰ Department of Physics and Astronomy, University of Sheffield, Sheffield, United Kingdom
¹⁴¹ Department of Physics, Shinshu University, Nagano, Japan
¹⁴² Fachbereich Physik, Universität Siegen, Siegen, Germany
¹⁴³ Department of Physics, Simon Fraser University, Burnaby BC, Canada
¹⁴⁴ SLAC National Accelerator Laboratory, Stanford CA, United States of America
¹⁴⁵ ^(a) Faculty of Mathematics, Physics & Informatics, Comenius University, Bratislava; ^(b) Department of Subnuclear Physics, Institute of Experimental Physics of the Slovak Academy of Sciences, Kosice, Slovak Republic
¹⁴⁶ ^(a) Department of Physics, University of Cape Town, Cape Town; ^(b) Department of Physics, University of Johannesburg, Johannesburg; ^(c) School of Physics, University of the Witwatersrand, Johannesburg, South Africa
¹⁴⁷ ^(a) Department of Physics, Stockholm University; ^(b) The Oskar Klein Centre, Stockholm, Sweden
¹⁴⁸ Physics Department, Royal Institute of Technology, Stockholm, Sweden
¹⁴⁹ Departments of Physics & Astronomy and Chemistry, Stony Brook University, Stony Brook NY, United States of America
¹⁵⁰ Department of Physics and Astronomy, University of Sussex, Brighton, United Kingdom
¹⁵¹ School of Physics, University of Sydney, Sydney, Australia
¹⁵² Institute of Physics, Academia Sinica, Taipei, Taiwan
¹⁵³ Department of Physics, Technion: Israel Institute of Technology, Haifa, Israel
¹⁵⁴ Raymond and Beverly Sackler School of Physics and Astronomy, Tel Aviv University, Tel Aviv, Israel
¹⁵⁵ Department of Physics, Aristotle University of Thessaloniki, Thessaloniki, Greece
¹⁵⁶ International Center for Elementary Particle Physics and Department of Physics, The University of Tokyo, Tokyo, Japan
¹⁵⁷ Graduate School of Science and Technology, Tokyo Metropolitan University, Tokyo, Japan
¹⁵⁸ Department of Physics, Tokyo Institute of Technology, Tokyo, Japan
¹⁵⁹ Department of Physics, University of Toronto, Toronto ON, Canada
¹⁶⁰ ^(a) TRIUMF, Vancouver BC; ^(b) Department of Physics and Astronomy, York University, Toronto ON, Canada
¹⁶¹ Faculty of Pure and Applied Sciences, University of Tsukuba, Tsukuba, Japan
¹⁶² Department of Physics and Astronomy, Tufts University, Medford MA, United States of America

- ¹⁶³ Centro de Investigaciones, Universidad Antonio Narino, Bogota, Colombia
- ¹⁶⁴ Department of Physics and Astronomy, University of California Irvine, Irvine CA, United States of America
- ¹⁶⁵ ^(a) INFN Gruppo Collegato di Udine, Sezione di Trieste, Udine; ^(b) ICTP, Trieste; ^(c) Dipartimento di Chimica, Fisica e Ambiente, Università di Udine, Udine, Italy
- ¹⁶⁶ Department of Physics, University of Illinois, Urbana IL, United States of America
- ¹⁶⁷ Department of Physics and Astronomy, University of Uppsala, Uppsala, Sweden
- ¹⁶⁸ Instituto de Física Corpuscular (IFIC) and Departamento de Física Atómica, Molecular y Nuclear and Departamento de Ingeniería Electrónica and Instituto de Microelectrónica de Barcelona (IMB-CNM), University of Valencia and CSIC, Valencia, Spain
- ¹⁶⁹ Department of Physics, University of British Columbia, Vancouver BC, Canada
- ¹⁷⁰ Department of Physics and Astronomy, University of Victoria, Victoria BC, Canada
- ¹⁷¹ Department of Physics, University of Warwick, Coventry, United Kingdom
- ¹⁷² Waseda University, Tokyo, Japan
- ¹⁷³ Department of Particle Physics, The Weizmann Institute of Science, Rehovot, Israel
- ¹⁷⁴ Department of Physics, University of Wisconsin, Madison WI, United States of America
- ¹⁷⁵ Fakultät für Physik und Astronomie, Julius-Maximilians-Universität, Würzburg, Germany
- ¹⁷⁶ Fachbereich C Physik, Bergische Universität Wuppertal, Wuppertal, Germany
- ¹⁷⁷ Department of Physics, Yale University, New Haven CT, United States of America
- ¹⁷⁸ Yerevan Physics Institute, Yerevan, Armenia
- ¹⁷⁹ Centre de Calcul de l'Institut National de Physique Nucléaire et de Physique des Particules (IN2P3), Villeurbanne, France
- ^a Also at Department of Physics, King's College London, London, United Kingdom
- ^b Also at Institute of Physics, Azerbaijan Academy of Sciences, Baku, Azerbaijan
- ^c Also at Novosibirsk State University, Novosibirsk, Russia
- ^d Also at Particle Physics Department, Rutherford Appleton Laboratory, Didcot, United Kingdom
- ^e Also at TRIUMF, Vancouver BC, Canada
- ^f Also at Department of Physics, California State University, Fresno CA, United States of America
- ^g Also at Department of Physics, University of Fribourg, Fribourg, Switzerland
- ^h Also at Departamento de Fisica e Astronomia, Faculdade de Ciencias, Universidade do Porto, Portugal
- ⁱ Also at Tomsk State University, Tomsk, Russia
- ^j Also at CPPM, Aix-Marseille Université and CNRS/IN2P3, Marseille, France
- ^k Also at Universita di Napoli Parthenope, Napoli, Italy
- ^l Also at Institute of Particle Physics (IPP), Canada
- ^m Also at Department of Physics, St. Petersburg State Polytechnical University, St. Petersburg, Russia
- ⁿ Also at Chinese University of Hong Kong, China
- ^o Also at Louisiana Tech University, Ruston LA, United States of America
- ^p Also at Institutio Catalana de Recerca i Estudis Avancats, ICREA, Barcelona, Spain
- ^q Also at Department of Physics, The University of Texas at Austin, Austin TX, United States of America
- ^r Also at Institute of Theoretical Physics, Ilia State University, Tbilisi, Georgia
- ^s Also at CERN, Geneva, Switzerland
- ^t Also at Georgian Technical University (GTU), Tbilisi, Georgia
- ^u Also at Ochadai Academic Production, Ochanomizu University, Tokyo, Japan
- ^v Also at Manhattan College, New York NY, United States of America
- ^w Also at Hellenic Open University, Patras, Greece
- ^x Also at Institute of Physics, Academia Sinica, Taipei, Taiwan
- ^y Also at LAL, Université Paris-Sud and CNRS/IN2P3, Orsay, France
- ^z Also at Academia Sinica Grid Computing, Institute of Physics, Academia Sinica, Taipei, Taiwan
- ^{aa} Also at School of Physics, Shandong University, Shandong, China
- ^{ab} Also at Laboratoire de Physique Nucléaire et de Hautes Energies, UPMC and Université Paris-Diderot and CNRS/IN2P3, Paris, France
- ^{ac} Also at School of Physical Sciences, National Institute of Science Education and Research,

Bhubaneswar, India

ad Also at Dipartimento di Fisica, Sapienza Università di Roma, Roma, Italy

ae Also at Moscow Institute of Physics and Technology State University, Dolgoprudny, Russia

af Also at Section de Physique, Université de Genève, Geneva, Switzerland

ag Also at International School for Advanced Studies (SISSA), Trieste, Italy

ah Also at Department of Physics and Astronomy, University of South Carolina, Columbia SC, United States of America

ai Also at School of Physics and Engineering, Sun Yat-sen University, Guangzhou, China

aj Also at Faculty of Physics, M.V.Lomonosov Moscow State University, Moscow, Russia

ak Also at National Research Nuclear University MEPhI, Moscow, Russia

al Also at Institute for Particle and Nuclear Physics, Wigner Research Centre for Physics, Budapest, Hungary

am Also at Department of Physics, Oxford University, Oxford, United Kingdom

an Also at Department of Physics, Nanjing University, Jiangsu, China

ao Also at Institut für Experimentalphysik, Universität Hamburg, Hamburg, Germany

ap Also at Department of Physics, The University of Michigan, Ann Arbor MI, United States of America

aq Also at Discipline of Physics, University of KwaZulu-Natal, Durban, South Africa

ar Also at University of Malaya, Department of Physics, Kuala Lumpur, Malaysia

* Deceased